

Fermion mass hierarchy and $g-2$ anomalies in an extended 3HDM Model

A. E. Cárcamo Hernández^{a,b,c,*}, Sergey Kovalenko^{b,c,d,†}, M. Maniatis^{e,‡} and Ivan Schmidt^{a,b,c,§}

^a *Universidad Técnica Federico Santa María,
Casilla 110-V, Valparaíso, Chile*

^b *Centro Científico-Tecnológico de Valparaíso,
Casilla 110-V, Valparaíso, Chile*

^c *Millennium Institute for Subatomic Physics at the High-Energy Frontier,
SAPHIR, Calle Fernández Concha No 700, Santiago, Chile*

^d *Departamento de Ciencias Físicas,
Universidad Andrés Bello,*

Sazié 2212, Piso 7, Santiago, Chile

^e *Departamento de Ciencias Básicas,
UBB, Casilla 447, Chillán, Chile,*

(Dated: October 13, 2021)

We propose an extension of the three-Higgs-doublet model (3HDM), where the Standard Model (SM) particle content is enlarged by the inclusion of two inert SU_{2L} scalar doublets, three inert and two active electrically neutral gauge singlet scalars, charged vector like fermions and Majorana neutrinos. These additional particles are introduced to generate the SM fermion mass hierarchy from a sequential loop suppression mechanism. In our model the top and exotic fermion masses appear at tree level, whereas the remaining fermions get their masses radiatively. Specifically, bottom, charm, tau and muon masses appear at 1-loop; the masses for the light up, down and strange quarks as well as for the electron at 2-loop and masses for the light active neutrinos at 3-loop. Our model successfully accounts for SM fermion masses and mixings and accommodates the observed Dark Matter relic density, the electron and muon anomalous magnetic moments, as well the constraints arising from charged Lepton Flavor Violating (LFV) processes. The proposed model predicts charged LFV decays within the reach of forthcoming experiments.

DOI:[10.1007/JHEP10\(2021\)036](https://doi.org/10.1007/JHEP10(2021)036)

I. INTRODUCTION

Despite the great consistency of the Standard Model with experimental data, it has several unexplained shortcomings. Among the most pressings are the absence of any explanation for the smallness of the masses of the neutrinos and the electron, and for the existence of three fermion families, accompanied by its mixing. The huge fermion mass hierarchy, which spreads over a range of 13 orders of magnitude, from the light neutrino mass scale up to the top quark mass, lacks any explanation. Moreover, there is no assertion for the smallness of the quark mixing angles, which contrasts with the sizable values of two of the three leptonic mixing angles.

To tackle the limitations of the SM, various extensions, including larger scalar and/or fermion sectors as well as extended symmetries, discrete and (or) continuous, with radiative seesaw mechanisms, have been proposed in the literature [1–88]. Furthermore, several theories with enlarged particle spectrum and symmetries have been constructed to explain the experimental value of the muon anomalous magnetic moment [69, 80, 84, 87–153], anomaly not explained by the SM and recently confirmed by the Muon $g - 2$ experiment at FERMILAB [154].

Recently, three of us proposed a model of fermion mass generation, where the fermion mass hierarchy arises from the

*Electronic address: antonio.carcamo@usm.cl

†Electronic address: sergey.kovalenko@unab.cl

‡Electronic address: maniatis8@gmail.com

§Electronic address: ivan.schmidt@usm.cl

sequential loop suppression, as follows [155]:

$$t\text{-quark} \rightarrow \text{tree-level mass from Yukawa couplings,} \quad (1)$$

$$b, c, \tau, \mu \rightarrow 1\text{-loop mass; tree-level} \quad (2)$$

suppressed by a *symmetry*.

$$s, u, d, e \rightarrow 2\text{-loop mass; tree-level \& 1-loop} \quad (3)$$

suppressed by a *symmetry*.

$$\nu_i \rightarrow n\text{-loop mass } (n > 2); \text{ tree-level \& lower loops} \quad (4)$$

suppressed by a *symmetry*.

with neutrino mass generated at 4-loop level ($n = 4$). However, this model has a low cutoff scale, since it includes non-renormalizable Yukawa terms, needed to implement the radiative mechanisms of the SM fermion mass generation (1)-(4). From the view-point of model building, it is much more preferable to have a renormalizable setup with a moderate amount of particle content and predicting a phenomenology beyond the SM within the reach of future experimental sensitivities. With this in mind, we propose here a renormalizable model implementing the sequential loop-suppression mechanism (1)-(3) with the light active neutrino masses appearing at three loop level ($n = 3$). This model has a much more economical field content compared to the similar renormalizable models proposed in Refs. [50, 79]. For instance, whereas the scalar sector of the model of Ref. [79] has 2 SU_{2L} scalar doublets, 7 complex electrically neutral gauge singlet scalars and 5 electrically charged singlet scalar fields, thus amounting to 32 scalar degrees of freedom, the model proposed here has three SU_{2L} scalar doublets, 3 complex and 2 real electrically neutral singlet scalars, which corresponds to 20 scalar degrees of freedom. Furthermore, the scalar sector of the model of Ref. [50] has three SU_{3L} scalar triplets, three complex electrically neutral singlet scalars and four electrically charged singlet scalar fields, thus amounting to 32 scalar degrees of freedom, which is much larger than the number of scalar degrees of freedom of our current model.

Moreover, our model can also successfully accommodate the electron and muon anomalous magnetic moments, the observed Dark Matter relic density, as well the constraints arising from charged Lepton Flavor Violating (LFV) processes.

Let us emphasize the difference of our proposed model with respect to recent publications based on radiative mass and hierarchy generation: In Ref. [156] there is no mechanism to generate the masses of the quarks of the first generation. In addition, the model described in [156] does not provide an explanation for the SM lepton mass hierarchy. In Ref. [157], both the first and second generation SM charged fermion masses are produced at one loop, whereas here we generate the lightest SM charged fermion masses at two loop level. Moreover, in [157] the neutrinos remain massless.

The paper is organized as follows. In section II we outline the proposed model. In section III we analyze the stability and describe the electroweak symmetry breaking of the scalar potential of the model. The scalar mass spectrum of the model is discussed in section IV. The implications of our model with respect to the SM fermion-mass hierarchy is discussed in section V. In section VI charged LFV decays as well as the constraints on the charged scalar masses are considered. The implications of our model for the muon and electron anomalous magnetic moments are discussed in section VII. The prospects with respect to Dark Matter are analyzed in section VIII. Our conclusions are given in section IX.

II. THE MODEL

Before providing a complete model setup, let us explain the motivations behind introducing extra scalars, fermions and symmetries needed for a consistent implementation of the sequential loop suppression mechanism for generating the SM fermion hierarchies.

Our strategy is to ban certain operators, by imposing appropriate symmetries to ensure loop suppression, necessary to reproduce the observable hierarchy of the SM fermion masses.

In our model the top quark mass arises at tree level from a renormalizable Yukawa operator, with an order one Yukawa coupling, i.e.

$$\bar{q}_{iL} \tilde{\phi} u_{3R}, \quad i = 1, 2, 3. \quad (5)$$

We denote the left-handed quarks by q_{iL} and the right-handed up and down quarks by u_{iR} and d_{iR} , respectively, with $i = 1, 2, 3$ the family index. The SM like Higgs boson doublet is denoted by ϕ .

To generate the bottom, charm, tau and muon masses at one loop level, it is necessary to forbid the operators:

$$\begin{aligned} \bar{f}_{iL} H f_R, \quad f_{iL} = q_{iL}, l_{iL}, \quad f_R = u_{2R}, d_{3R}, l_{2R}, l_{3R}, \\ i = 1, 2, 3, \quad \text{with } H = \begin{cases} \tilde{\phi} & \text{for } f_R = u_{2R}, \\ \phi & \text{for } f_R = d_{3R}, l_{2R}, l_{3R}. \end{cases}, \end{aligned} \quad (6)$$

at tree level and to allow the following operators, crucial to close the one loop level diagram of the upper left panel of Figure 1:

$$\begin{aligned} \bar{f}_{iL} \Phi F_{rR}, \quad \bar{F}_{rL} \sigma f_R, \quad f_{iL} = q_{iL}, l_{iL}, \quad f_R = u_{2R}, d_{3R}, l_{2R}, l_{3R}, \\ i = 1, 2, 3, \quad r = \begin{cases} 1 & \text{for quarks,} \\ 2 & \text{for charged leptons.} \end{cases}, \quad \Phi = \begin{cases} \tilde{\eta} & \text{for } f_R = u_{2R}, \\ \eta & \text{for } f_R = d_{3R}, l_{2R}, l_{3R}. \end{cases}, \\ A \left[(\phi^\dagger \eta) \sigma + h.c. \right], \quad (y_F)_r \bar{F}_{rL} \chi F_{rR} \end{aligned} \quad (7)$$

This requires to add an unbroken $Z_2^{(2)}$ symmetry as well as a spontaneously broken $Z_2^{(1)}$ symmetry. Under the spontaneously broken $Z_2^{(1)}$ symmetry, all the right handed SM fermionic fields, excepting u_{3R} are charged. Under this $Z_2^{(1)}$ symmetry, the singlet scalar field χ as well as the left-handed exotic fermionic field F_{rL} are charged. Furthermore, all SM fermionic fields are neutral under the unbroken $Z_2^{(2)}$ symmetry whereas the left-handed and right-handed exotic fermionic fields F_{rL} and F_{rR} are charged under $Z_2^{(2)}$. The inclusion of the spontaneously broken $Z_2^{(1)}$ and unbroken $Z_2^{(2)}$ symmetries is crucial for the implementation of the radiative seesaw mechanism that produces one-loop level masses for the bottom, charm, tau and muon without invoking soft-breaking mass terms. Notice that the fermionic sector is enlarged by electroweak charged exotic fermions F_r , where $r = 1$ for quarks and $r = 2$ for charged leptons, and that the Yukawa operators as well as the trilinear scalar operator shown in Eq. (7) correspond to the three vertices of the one loop level diagram in the upper left panel of Figure 1. Considering the simplest possibility, where such charged exotic fermions F_r are SU_{2L} singlets, the scalar sector has to be extended by the inclusion of an extra SU_{2L} scalar doublet η and an electrically neutral electroweak gauge-singlet scalars σ and χ . The scalar fields η and σ are both charged under the preserved $Z_2^{(2)}$ symmetry, whereas the scalar χ is neutral under this symmetry. The singlet scalar field χ is needed to provide masses to the charged exotic fermions F_r . This scalar field χ is assumed to be charged under the spontaneously broken $Z_2^{(1)}$ symmetry. Furthermore, the Yukawa term $(y_F)_r \bar{F}_{rL} \chi F_{rR}$, which involves the electroweak charged exotic fermions, must also be included as well, in order to close the one loop level diagram of Figure 1.

Besides that, small masses for the light SM charged fermions, i.e., the up, down and strange quarks as well as the electron, are generated at two loop level. This implies to forbid the following operators that would give rise to tree and one-loop-level masses for these particles:

$$\begin{aligned} \bar{f}_{iL} H f_R, \quad f_{iL} = q_{iL}, l_{iL}, \quad f_R = u_{1R}, d_{1R}, d_{2R}, l_{1R}, \quad i = 1, 2, 3, \\ H = \begin{cases} \tilde{\phi} & \text{for } f_R = u_{1R}, \\ \phi & \text{for } f_R = d_{1R}, d_{2R}, l_{1R}. \end{cases}, \\ \bar{f}_{iL} \Phi F_{rR}, \quad \bar{F}_{rL} \sigma f_R, \quad f_{iL} = q_{iL}, l_{iL}, \quad f_R = u_{1R}, d_{1R}, d_{2R}, l_{1R}, \\ i = 1, 2, 3, \quad r = \begin{cases} 1 & \text{for quarks,} \\ 2 & \text{for charged leptons.} \end{cases}, \quad \Phi = \begin{cases} \tilde{\eta} & \text{for } f_R = u_{2R}, \\ \eta & \text{for } f_R = d_{3R}, l_{2R}, l_{3R}. \end{cases} \end{aligned} \quad (8)$$

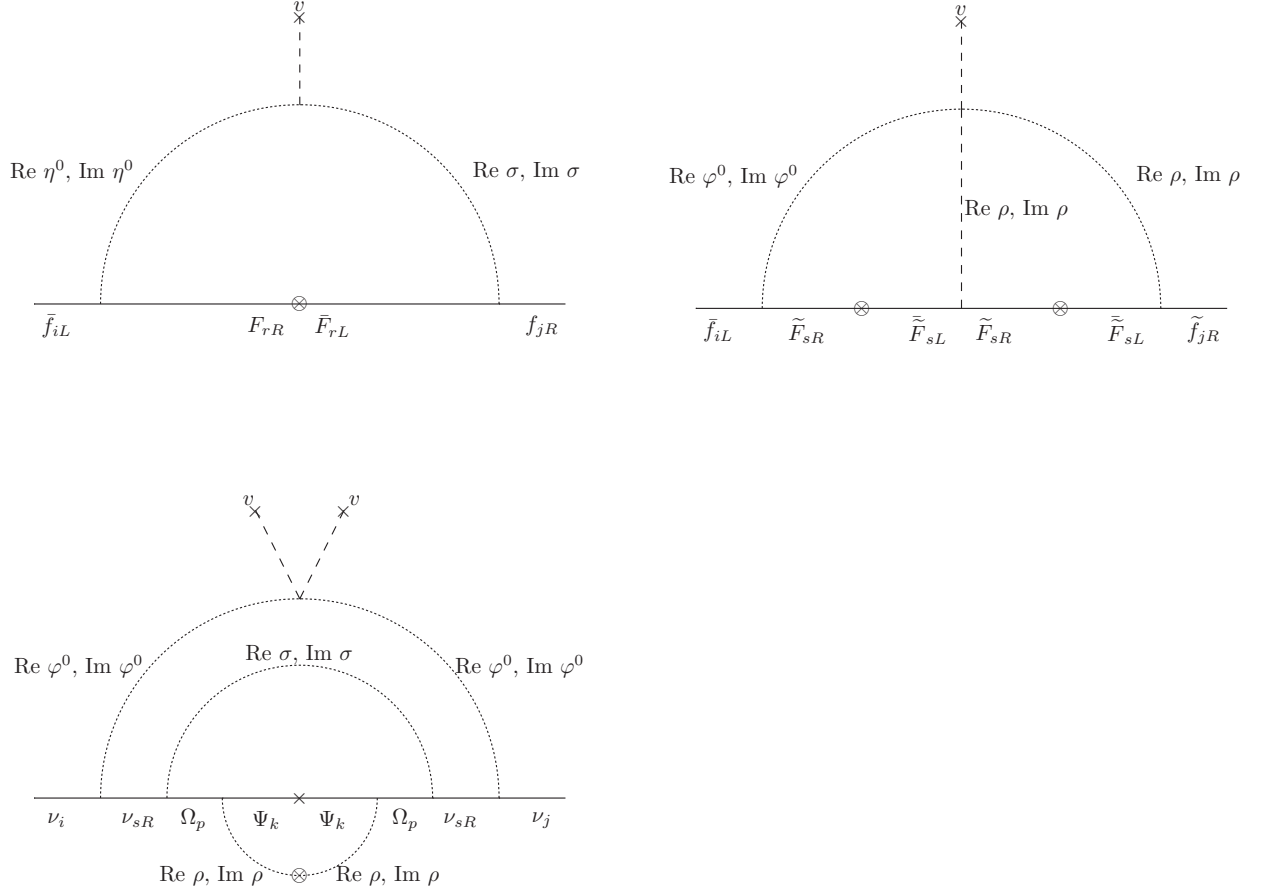


Figure 1: Loop diagrams contributing to the fermion mass matrices. Here $f_{iL} = u_{iL}, d_{iL}, e_{iL}$ ($i = 1, 2, 3$), $f_R = u_{2R}, d_{3R}, l_{2R}, l_{3R}$, $f_R = u_{1R}, d_{1R}, d_{2R}, l_{1R}$. The electroweak singlet charged exotic fermions, see (13), are denoted by F_{rR} , F_{rL} , \tilde{F}_{sR} and \tilde{F}_{sL} , where $r = 1$ for quarks, $r = 2$ for charged leptons, $s = 1$ for up type quarks and charged leptons, and $s = 2$ for down type quarks and neutrinos. Furthermore, in the neutrino loop diagram we have $p, k \in \{1, 2\}$.

However the following operators are required to provide two loop level masses for the light SM charged fermions:

$$\begin{aligned}
& \bar{f}_{iL} \Xi \tilde{F}_{sR}, \quad \bar{\tilde{F}}_{sL} \Delta \tilde{F}'_{sR}, \quad \bar{\tilde{F}}'_{sL} \zeta \tilde{F}'_{sR}, \quad \bar{\tilde{F}}'_{sL} \Theta \tilde{f}_R, \\
& f_{iL} = q_{iL}, l_{iL}, \quad \Xi = \begin{cases} \tilde{\varphi} & \text{for } f_R = u_{1R}, \\ \varphi & \text{for } f_R = d_{1R}, d_{2R}, l_{1R}. \end{cases}, \quad \tilde{f}_R = u_{1R}, d_{1R}, d_{2R}, l_{1R}, \quad i = 1, 2, 3 \\
& \Theta = \begin{cases} \xi^* & \text{for } f_R = u_{1R}, d_{1R}, d_{2R} \\ \xi & \text{for } f_R = l_{1R}. \end{cases}, \quad \Delta = \begin{cases} \rho^* & \text{for } \tilde{F}_{sL} = \tilde{T}_L, \tilde{B}_{sL} \\ \rho & \text{for } \tilde{F}_{sL} = \tilde{E}_L. \end{cases}, \\
& \left[(\phi^\dagger \varphi) \rho \xi + h.c. \right], \quad (m_{\tilde{F}})_s \bar{\tilde{F}}_{sL} \tilde{F}_{sR}, \quad (y_{\tilde{F}'})_s \bar{\tilde{F}}'_{sL} \zeta \tilde{F}'_{sR}, \\
& s = \begin{cases} 1 & \text{for up-type quarks and charged leptons,} \\ 2 & \text{for down-type quarks.} \end{cases} \tag{9}
\end{aligned}$$

Such operators are crucial to close the two-loop-level diagram of the upper right panel of Figure 1. For this to happen, the fermion sector is extended as well, by adding the electroweak charged exotic fermions $\tilde{F}_s, \tilde{F}'_s$ where $s = 1$ for up-type quarks and charged exotic leptons and $s = 2$ for down-type quarks. The simplest choice is to assign these charged exotic fermions $\tilde{F}_s, \tilde{F}'_s$ to SU_{2L} singlets. Then, in order to build the Yukawa interactions that determine three of the four vertices of the two loop level diagram of Figure 1, we also need to add an extra SU_{2L} scalar doublet φ and another electrically neutral electroweak gauge-singlet scalars ρ, ξ and ζ . The scalar fields φ, ρ and ξ are assumed to have complex charges under an additional spontaneously broken Z_4 symmetry, whereas the scalar ζ has a real charge under this Z_4 symmetry. We further assume that the Z_4 symmetry is spontaneously broken down to a preserved Z_2 symmetry, which implies that the scalar fields ρ and ξ do not acquire vacuum expectation values whereas the scalar ζ does. Furthermore, in order to close the aforementioned two loop diagram, one has to include the mass term $(m_{\tilde{F}})_s \tilde{F}_{sL} \tilde{F}_{sR}$ and the Yukawa interaction $(y_{\tilde{F}})_s \tilde{F}'_{sL} \zeta \tilde{F}'_{sR}$ involving the electroweakly charged exotic fermions. Notice that the Yukawa operators, as well as the quartic scalar operator shown in Eq. (9), correspond to the four vertices of the two loop level diagram of the upper right panel of Figure 1.

In what regards the neutrino sector, we require that the light active neutrino masses only appear at three-loop level. To this end, right-handed Majorana-neutrinos have to be added in the fermionic spectrum. In addition, one should prevent the appearance of tree, one and two-loop level masses for the light active neutrinos. Generating light active neutrino masses at three-loop level, as in the Feynman diagram of the bottom left panel of Figure 1, requires the presence of the operators

$$\bar{l}_{jL} \tilde{\varphi} \nu_{sR}, \quad \overline{\nu_{sR}^C} \sigma \Omega_{pR}, \quad \overline{\nu_{sR}^C} \sigma \Omega_{pR}, \quad \overline{\Omega_{sR}^C} \rho \Psi_{pR}, \quad (m_{\Psi})_{sp} \Psi_{sR} \overline{\Psi_{pR}^C}, \quad (\rho^2 \chi \zeta + h.c.), \quad (10)$$

and forbidding:

$$\bar{l}_{jL} \phi \nu_{sR}, \quad m_N \nu_{sR} \overline{\nu_{sR}^C}, \quad \bar{l}_{jL} \tilde{\eta} \nu_{sR}, \quad (m_{\Omega})_{sp} \Omega_{sR} \overline{\Omega_{pR}^C}, \quad (11)$$

where ν_{sR}, Ω_{sR} and Ψ_{sR} ($s = 1, 2$) are gauge singlet right-handed Majorana neutrinos. By an appropriate choice of charges (shown below) under the aforementioned $Z_2^{(1)} \times Z_2^{(2)} \times Z_4$ symmetry, the three-loop level radiative seesaw mechanism for light active neutrinos can be implemented.

With the aim of implementing the sequential loop suppression mechanism that generates the pattern of SM fermion masses, we consider an extension of the inert 3HDM, where the SM gauge symmetry is supplemented by a $Z_2^{(1)} \times Z_2^{(2)} \times Z_4$ discrete symmetry and the scalar sector is extended to include five SM scalar singlets, i.e., σ, ρ, ξ, χ and ζ . The reason to consider this extra $Z_2^{(1)} \times Z_2^{(2)} \times Z_4$ discrete symmetry is that it is the smallest cyclic symmetry that allows us to realize the loop-suppression scenario (1)-(4) with $n = 3$ in a renormalizable 3HDM setup without invoking soft symmetry breaking.

The scalar sector of the model consists of three SU_{2L} scalar doublets, i.e., ϕ, η, φ and five scalar singlets σ, ρ, ξ, χ and ζ , with the $Z_2^{(1)} \times Z_2^{(2)} \times Z_4$ assignments:

$$\begin{aligned} \phi &\sim (1, 1, 1), & \eta &\sim (1, -1, 1), & \varphi &\sim (1, -1, -1), & \sigma &\sim (1, -1, 1), & \rho &\sim (1, -1, -i), \\ \xi &\sim (1, 1, -i), & \chi &\sim (-1, 1, 1), & \zeta &\sim (-1, 1, -1) \end{aligned} \quad (12)$$

We assume that the $Z_2^{(2)}$ symmetry is unbroken whereas the $Z_2^{(1)}$ and Z_4 symmetries are spontaneously broken. We further assume that the Z_4 symmetry is spontaneously broken down to a preserved Z_2 symmetry. These assumptions imply that the scalar fields $\eta, \varphi, \sigma, \rho, \xi$, charged under the $Z_2^{(2)}$ symmetry and (or) having complex Z_4 charges, do not acquire vacuum expectation values. This conditions are inevitable in the present setup for implementing the scenario (1)-(4). Let us note that the SU_{2L} scalar doublet ϕ is the only scalar field that acquires a non-vanishing vacuum expectation value (VEV) equal to about 246 GeV and thus corresponds to the SM Higgs doublet.

A justification of the extension of the scalar sector of the model is provided in the following. The SU_{2L} inert scalar doublet η as well as the inert SM gauge singlet scalar σ are introduced to generate the one-loop level masses for the bottom, charm quarks, tau and muon leptons. The scalar singlets χ and ζ are introduced to provide masses to the charged exotic fermions. Moreover, the implementation of the two-loop level radiative seesaw mechanisms, generating the up, down, strange quark masses as well as the electron mass, requires to introduce an extra SU_{2L} inert scalar doublet, namely φ and inert SM gauge singlet scalars, i.e., ρ and ξ . The particles φ and ρ are also crucial to give three-loop level masses for the light active neutrinos. The three loop level neutrino mass diagram is closed thanks to the gauge singlet scalars χ and ζ .

The fermion sector of the SM is extended by the SU_{2L} singlet exotic quarks $T, \tilde{T}, \tilde{T}', B, \tilde{B}, \tilde{B}'$ and singlet leptons $E, \tilde{E}, \tilde{E}', \nu_s$ ($s = 1, 2$), Ω, Ψ with electric charges $Q(T) = Q(\tilde{T}) = 2/3, Q(B) = Q(\tilde{B}) = -1/3, Q(E) = -1$. The

$Z_2^{(1)} \times Z_2^{(2)} \times Z_4$ assignments of the fermion sector are:

$$\begin{aligned}
u_{1R} &\sim (-1, 1, -1), & u_{2R} &\sim (-1, 1, 1), & u_{3R} &\sim (1, 1, 1), \\
d_{1R} &\sim (-1, 1, -1), & d_{2R} &\sim (-1, 1, -1), & d_{3R} &\sim (-1, 1, 1), \\
l_{1R} &\sim (-1, 1, -i), & l_{2R} &\sim (-1, 1, i), & l_{3R} &\sim (-1, 1, i), \\
q_{jL} &\sim (1, 1, 1), & l_{jL} &\sim (1, 1, i), & j &= 1, 2, 3, \\
T_L &\sim (-1, -1, 1), & T_R &\sim (1, -1, 1), & \tilde{T}_L &\sim (1, -1, -1), & \tilde{T}_R &\sim (1, -1, -1), \\
\tilde{T}'_L &\sim (-1, 1, -i), & \tilde{T}'_R &\sim (1, 1, i), & B_L &\sim (-1, -1, 1), & B_R &\sim (1, -1, 1), \\
B_L &\sim (-1, -1, 1), & B_R &\sim (1, -1, 1), & \tilde{B}_{sL} &\sim (1, -1, -1), & \tilde{B}_{sR} &\sim (1, -1, -1), \\
\tilde{B}'_L &\sim (-1, 1, -i), & \tilde{B}'_R &\sim (1, 1, i), & E_{sL} &\sim (-1, -1, i), & E_{sR} &\sim (1, -1, i), \\
\tilde{E}_L &\sim (1, -1, -i), & \tilde{E}_R &\sim (1, -1, -i), & \tilde{E}'_L &\sim (-1, 1, -1), & \tilde{E}'_R &\sim (1, 1, 1), \\
\nu_{sR} &\sim (1, -1, -i), & s &= 1, 2, & \Omega_{sR} &\sim (1, 1, i), & \Psi_{sR} &\sim (1, -1, 1).
\end{aligned} \tag{13}$$

The quark, lepton and scalar assignments under $SU_{3c} \times SU_{2L} \times U_{1Y} \times Z_2^{(1)} \times Z_2^{(2)} \times Z_4$ are shown in Tables I, II and III, respectively.

	q_{jL}	u_{1R}	u_{2R}	u_{3R}	d_{1R}	d_{2R}	d_{3R}	T_L	T_R	\tilde{T}_L	\tilde{T}_R	\tilde{T}'_L	\tilde{T}'_R	B_L	B_R	\tilde{B}_{sL}	\tilde{B}_{sR}	\tilde{B}'_{sL}	\tilde{B}'_{sR}	
SU_{3c}	3	3	3	3	3	3	3	3	3	3	3	3	3	3	3	3	3	3	3	3
SU_{2L}	2	1	1	1	1	1	1	1	1	1	1	1	1	1	1	1	1	1	1	1
U_{1Y}	$\frac{1}{6}$	$\frac{2}{3}$	$\frac{2}{3}$	$\frac{2}{3}$	$-\frac{1}{3}$	$-\frac{1}{3}$	$-\frac{1}{3}$	$\frac{2}{3}$	$\frac{2}{3}$	$\frac{2}{3}$	$\frac{2}{3}$	$\frac{2}{3}$	$\frac{2}{3}$	$-\frac{1}{3}$	$-\frac{1}{3}$	$-\frac{1}{3}$	$-\frac{1}{3}$	$-\frac{1}{3}$	$-\frac{1}{3}$	$-\frac{1}{3}$
$Z_2^{(1)}$	1	-1	-1	1	-1	-1	-1	-1	1	1	1	-1	1	-1	1	1	1	-1	1	1
$Z_2^{(2)}$	1	1	1	1	1	1	1	-1	-1	-1	-1	1	1	-1	-1	-1	-1	1	1	1
Z_4	1	-1	1	1	-1	-1	1	1	1	-1	-1	-i	i	1	1	-1	-1	-i	i	i

Table I: Quark assignments under $SU_{3c} \times SU_{2L} \times U_{1Y} \times Z_2^{(1)} \times Z_2^{(2)} \times Z_4$. Here $j = 1, 2, 3$ and $s = 1, 2$.

	l_{jL}	l_{1R}	l_{2R}	l_{3R}	E_{sL}	E_{sR}	\tilde{E}_L	\tilde{E}_R	\tilde{E}'_L	\tilde{E}'_R	ν_{sR}	Ω_{sR}	Ψ_{sR}
SU_{3c}	1	1	1	1	1	1	1	1	1	1	1	1	1
SU_{2L}	2	1	1	1	1	1	1	1	1	1	1	1	1
U_{1Y}	$-\frac{1}{2}$	-1	-1	-1	-1	-1	-1	-1	-1	-1	0	0	0
$Z_2^{(1)}$	1	-1	-1	-1	-1	1	1	1	-1	1	1	1	1
$Z_2^{(2)}$	1	1	1	1	-1	-1	-1	-1	1	1	-1	1	-1
Z_4	i	$-i$	i	i	i	i	$-i$	$-i$	-1	1	$-i$	i	1

Table II: Lepton assignments under $SU_{3c} \times SU_{2L} \times U_{1Y} \times Z_2^{(1)} \times Z_2^{(2)} \times Z_4$. Here $j = 1, 2, 3$ and $s = 1, 2$.

	ϕ	η	φ	σ	ρ	ξ	χ	ζ
SU_{3c}	1	1	1	1	1	1	1	1
SU_{2L}	2	2	2	1	1	1	1	1
U_{1Y}	$\frac{1}{2}$	$\frac{1}{2}$	$\frac{1}{2}$	0	0	0	0	0
$Z_2^{(1)}$	1	1	1	1	1	1	-1	-1
$Z_2^{(2)}$	1	-1	-1	-1	-1	1	1	1
Z_4	1	1	-1	1	$-i$	$-i$	1	-1

Table III: Scalar assignments under $SU_{3c} \times SU_{2L} \times U_{1Y} \times Z_2^{(1)} \times Z_2^{(2)} \times Z_4$.

Now, let us justify the exotic fermion content of our model. The gauge-singlet neutral leptons ν_s , Ω_s , Ψ_s ($s = 1, 2$) are introduced to generate the three-loop level masses for two light active neutrinos. Let us note that the neutrino oscillation experimental data requires to have at least two light massive active neutrinos [158]. Furthermore, note that the SU_{2L} singlet exotic quarks T , \tilde{T} , \tilde{T}' , B , \tilde{B} , \tilde{B}' and singlet leptons E_s ($s = 1, 2$), \tilde{E} , \tilde{E}' introduced in our

model, correspond to the minimal amount of charged exotic fermion content needed to yield one-loop level masses for the bottom, charm quarks, tau and muon leptons, as well as two-loop level masses for the light up, down, strange quarks and the electron, without including soft-breaking mass terms.

With the specified particle content, we have the following quark, charged lepton and neutrino Yukawa terms invariant under the $Z_2^{(1)} \times Z_2^{(2)} \times Z_4$ discrete symmetry

$$\begin{aligned}
-\mathcal{L}_Y^{(U)} &= \sum_{j=1}^3 y_j^{(u)} \bar{q}_{jL} \tilde{\varphi} \tilde{T}_R + x^{(u)} \tilde{T}'_L \xi^* u_{1R} + \sum_{j=1}^3 z_j^{(u)} \bar{q}_{jL} \tilde{\eta} T_R + w^{(u)} \bar{T}_L \sigma u_{2R} \\
&+ \sum_{j=1}^3 y_{j3}^{(u)} \bar{q}_{jL} \tilde{\phi} u_{3R} + y_T \bar{T}_L \chi T_R + \tilde{m}_T \bar{T}_L \tilde{T}_R + y_{\tilde{T}'} \tilde{T}'_L \zeta \tilde{T}'_R + z_{\tilde{T}'} \bar{\tilde{T}'_L} \rho^* \tilde{T}'_R + h.c., \tag{14}
\end{aligned}$$

$$\begin{aligned}
-\mathcal{L}_Y^{(D)} &= \sum_{j=1}^3 \sum_{s=1}^2 y_{js}^{(d)} \bar{q}_{jL} \varphi \tilde{B}_{sR} + \sum_{s=1}^2 \sum_{k=1}^2 x_{sk}^{(d)} \tilde{B}'_{sL} \xi^* d_{kR} + \sum_{j=1}^3 z_j^{(d)} \bar{q}_{jL} \eta B_R + w^{(d)} \bar{B}_L \sigma d_{3R} \\
&+ y_B \bar{B}_L \chi B_R + \sum_{s=1}^2 \tilde{m}_{B_s} \bar{\tilde{B}}_{sL} \tilde{B}_{sR} + \sum_{s=1}^2 (y_{\tilde{B}'})_s \tilde{B}'_{sL} \zeta \tilde{B}'_{sR} + \sum_{s=1}^2 (x_{\tilde{B}'})_s \bar{\tilde{B}}_{sL} \rho^* \tilde{B}'_{sR} + h.c., \tag{15}
\end{aligned}$$

$$\begin{aligned}
-\mathcal{L}_Y^{(l)} &= \sum_{j=1}^3 y_j^{(l)} \bar{l}_{jL} \varphi \tilde{E}_R + x_1^{(l)} \tilde{E}'_L \xi l_{1R} + \sum_{j=1}^3 \sum_{s=1}^2 y_{js}^{(l)} \bar{l}_{jL} \eta E_{sR} + \sum_{s=1}^2 \sum_{k=2}^3 x_{sk}^{(l)} \bar{E}_{sL} \sigma l_{kR} \\
&+ \sum_{s=1}^2 y_{E_s} \bar{E}_{sL} \chi E_{sR} + \tilde{m}_E \bar{E}_L \tilde{E}_R + y_{\tilde{E}'} \tilde{E}'_L \zeta \tilde{E}'_R + z_{\tilde{E}'} \bar{\tilde{E}'_L} \rho \tilde{E}'_R + h.c., \tag{16}
\end{aligned}$$

$$-\mathcal{L}_Y^{(\nu)} = \sum_{j=1}^3 \sum_{s=1}^2 y_{js}^{(\nu)} \bar{l}_{jL} \tilde{\varphi} \nu_{sR} + \sum_{s=1}^2 \sum_{p=1}^2 y_{sp}^{(\nu)} \nu_{sR}^C \sigma \Omega_{pR} + \sum_{s=1}^2 \sum_{p=1}^2 y_{sp}^{(\Omega)} \bar{\Omega}_{sR}^C \rho \Psi_{pR} + \sum_{s=1}^2 \sum_{p=1}^2 (m_\Psi)_{sp} \Psi_{sR} \bar{\Psi}_{pR}^C + h.c. \tag{17}$$

After electroweak gauge-symmetry breaking, the above-given Yukawa interactions yield the SM fermion masses via sequential loop suppression. Furthermore, the non SM-like scalars (excepting the scalar singlets χ and ζ) are not allowed to acquire VEVs for the following reasons: Firstly, in this way we avoid to generate tree-level masses for the SM fermions lighter than the top quark. Secondly, we open the possibility to have stable scalar Dark Matter candidates. Eventually we also avoid to encounter tree level Flavor Changing Neutral Currents (FCNCs).

III. STABILITY AND ELECTROWEAK SYMMETRY BREAKING OF THE HIGGS POTENTIAL

The renormalizable Higgs potential, invariant under the symmetries of the model, has the form:

$$\begin{aligned}
V = & \mu_1^2 (\phi^\dagger \phi) + \mu_2^2 (\eta^\dagger \eta) + \mu_3^2 (\varphi^\dagger \varphi) + \mu_4^2 |\sigma|^2 + [\mu_5^2 \sigma^2 + h.c.] + \mu_6^2 |\rho|^2 + \mu_7^2 |\xi|^2 + \mu_8^2 \chi^2 + \mu_9^2 \zeta^2 \\
& + \lambda_1 (\phi^\dagger \phi)^2 + \lambda_2 (\eta^\dagger \eta)^2 + \lambda_3 (\varphi^\dagger \varphi)^2 + \lambda_4 (\phi^\dagger \phi) (\eta^\dagger \eta) + \lambda_5 (\phi^\dagger \phi) (\varphi^\dagger \varphi) \\
& + \lambda_6 (\eta^\dagger \eta) (\varphi^\dagger \varphi) + \lambda_7 (\phi^\dagger \eta) (\eta^\dagger \phi) + \lambda_8 (\phi^\dagger \varphi) (\varphi^\dagger \phi) + \lambda_9 (\eta^\dagger \varphi) (\varphi^\dagger \eta) \\
& + \left[\frac{\lambda_{10}}{2} (\phi^\dagger \eta)^2 + h.c. \right] + \left[\frac{\lambda_{11}}{2} (\phi^\dagger \varphi)^2 + h.c. \right] + \left[\frac{\lambda_{12}}{2} (\eta^\dagger \varphi)^2 + h.c. \right] \\
& + \kappa_1 |\sigma|^4 + \kappa_2 |\rho|^4 + \kappa_3 |\xi|^4 + \kappa_4 \chi^4 + \kappa_5 \zeta^4 + \kappa_6 |\sigma|^2 |\rho|^2 + \kappa_7 |\sigma|^2 |\xi|^2 + \kappa_8 |\rho|^2 |\xi|^2 \\
& + \kappa_9 |\rho|^2 |\xi|^2 + \kappa_{10} \chi^2 \zeta^2 + \kappa_{11} |\sigma|^2 \chi^2 + \kappa_{12} |\rho|^2 \chi^2 + \kappa_{13} |\xi|^2 \chi^2 + \kappa_{14} |\sigma|^2 \zeta^2 + \kappa_{15} |\rho|^2 \zeta^2 \\
& + \kappa_{16} |\xi|^2 \zeta^2 + \kappa_{17} (\rho^2 \zeta \chi + h.c.) + \kappa_{18} (\xi^2 \zeta \chi + h.c.) + \alpha_1 (\phi^\dagger \phi) |\sigma|^2 + [\alpha_2 \sigma^2 + h.c.] (\phi^\dagger \phi) \\
& + \alpha_3 (\phi^\dagger \phi) |\rho|^2 + \alpha_4 (\phi^\dagger \phi) |\xi|^2 + \alpha_5 (\eta^\dagger \eta) |\sigma|^2 + [\alpha_6 \sigma^2 + h.c.] (\eta^\dagger \eta) + \alpha_7 (\eta^\dagger \eta) |\rho|^2 \\
& + \alpha_8 (\eta^\dagger \eta) |\xi|^2 + \alpha_9 (\varphi^\dagger \varphi) |\sigma|^2 + [\alpha_{10} \sigma^2 + h.c.] (\varphi^\dagger \varphi) + \alpha_{11} (\varphi^\dagger \varphi) |\rho|^2 + \alpha_{12} (\varphi^\dagger \varphi) |\xi|^2 \\
& + \alpha_{13} (\phi^\dagger \phi) \chi^2 + \alpha_{14} (\phi^\dagger \phi) \zeta^2 + \alpha_{15} (\eta^\dagger \eta) \chi^2 + \alpha_{16} (\eta^\dagger \eta) \zeta^2 + \alpha_{17} (\varphi^\dagger \varphi) \chi^2 + \alpha_{18} (\varphi^\dagger \varphi) \zeta^2 \\
& + [A (\phi^\dagger \eta) \sigma + h.c.] + [B (\rho^* \xi) \sigma + h.c.] + \gamma [(\phi^\dagger \eta) \rho^* \xi + h.c.] + \varkappa [(\phi^\dagger \varphi) \rho \xi + h.c.]. \tag{18}
\end{aligned}$$

The scalar fields can be written as

$$\phi = \begin{pmatrix} \phi^+ \\ \frac{1}{\sqrt{2}} (v + \phi_R^0 + i\phi_I^0) \end{pmatrix}, \quad \eta = \begin{pmatrix} \eta^+ \\ \frac{1}{\sqrt{2}} (\eta_R^0 + i\eta_I^0) \end{pmatrix}, \quad \varphi = \begin{pmatrix} \varphi^+ \\ \frac{1}{\sqrt{2}} (\varphi_R^0 + i\varphi_I^0) \end{pmatrix}, \tag{19}$$

$$\sigma = \frac{1}{\sqrt{2}} (\sigma_R + i\sigma_I), \quad \rho = \frac{1}{\sqrt{2}} (\rho_R + i\rho_I), \quad \xi = \frac{1}{\sqrt{2}} (\xi_R + i\xi_I), \quad \chi = v_\chi + \tilde{\chi}, \quad \zeta = v_\zeta + \tilde{\zeta}. \tag{20}$$

From the condition to have a vanishing gradient of the potential with the neutral component of the doublet ϕ getting a VEV $v/\sqrt{2}$ as well as the scalar singlets χ, ζ acquiring VEVs v_χ and v_ζ , respectively, whereas all other VEVs are vanishing, we find the constraints on the potential parameters:

$$\mu_1^2 = -\lambda_1 v^2 - \alpha_{13} v_\chi^2 - \alpha_{14} v_\zeta^2, \tag{21}$$

$$\mu_8^2 = -2\kappa_4 v_\chi^2 - \kappa_{10} v_\zeta^2 - \alpha_{13} \frac{v^2}{2}, \tag{22}$$

$$\mu_9^2 = -2\kappa_5 v_\zeta^2 - \kappa_{10} v_\chi^2 - \alpha_{14} \frac{v^2}{2}, \tag{23}$$

From the symmetry of the potential (18) we find that for positive quartic parameters $\lambda_1, \lambda_2, \lambda_3$, as well as $\kappa_1, \kappa_2, \kappa_3, \kappa_4, \kappa_5$, the potential is bounded from below, that is, it is stable. However, we also have to ensure that it provides the experimentally acceptable electroweak symmetry breaking of $SU(2)_L \times U(1)_Y \rightarrow U(1)_{\text{em}}$ and gives the correct VEV of about $v \approx 246$ GeV.

Let us emphasize that in general it is not sufficient to check that the potential has a vanishing gradient, leading to the condition (21).

In particular, the corresponding local stationary point can correspond to a saddle point or maximum, and not a minimum. Moreover, there can be deeper stationary points. A systematic approach to find the global minimum for any 3HDM has been presented in [159]. The case of two Higgs-boson doublets accompanied by an arbitrary number of Higgs-boson singlets has been also studied [160]. For the potential considered here we have, in addition to the three Higgs-boson doublet fields ϕ, η, φ , also three complex singlet fields, σ, ρ and ξ and two real scalars χ and ζ . We adopt the formalism of three doublets presented in [159] to the case of additional Higgs-singlet fields that we have here.

The essential step is to introduce *bilinears* for the Higgs-boson doublets [161, 162] and decompose the complex Higgs singlets into its real and imaginary parts. First, all gauge-invariant scalar products of the three doublet fields ϕ, η, φ

are arranged in a matrix,

$$\underline{K} = \begin{pmatrix} \phi^\dagger\phi & \eta^\dagger\phi & \varphi^\dagger\phi \\ \phi^\dagger\eta & \eta^\dagger\eta & \varphi^\dagger\eta \\ \phi^\dagger\varphi & \eta^\dagger\varphi & \varphi^\dagger\varphi \end{pmatrix}. \quad (24)$$

This matrix can be expressed in a basis of matrices λ_α ($\alpha = 0, 1, \dots, 8$), where $\lambda_0 = \sqrt{\frac{2}{3}}\mathbb{1}_3$ is the conveniently scaled identity matrix and λ_a ($a = 1, \dots, 8$) are the Gell-Mann matrices. In this basis we can write

$$\underline{K} = \frac{1}{2} \sum_{\alpha=0}^8 K_\alpha \lambda_\alpha. \quad (25)$$

The real coefficients, called *bilinears* K_α , are obtained from

$$K_\alpha = K_\alpha^* = \text{tr}(\underline{K}\lambda_\alpha), \quad \alpha = 0, \dots, 8. \quad (26)$$

We can invert this relation and express the gauge-invariant scalar products of the doublets, which appear in the potential, in terms of the bilinears:

$$\begin{aligned} \phi^\dagger\phi &= \frac{K_0}{\sqrt{6}} + \frac{K_3}{2} + \frac{K_8}{2\sqrt{3}}, & \phi^\dagger\eta &= \frac{1}{2}(K_1 + iK_2), & \phi^\dagger\varphi &= \frac{1}{2}(K_4 + iK_5), \\ \eta^\dagger\eta &= \frac{K_0}{\sqrt{6}} - \frac{K_3}{2} + \frac{K_8}{2\sqrt{3}}, & \eta^\dagger\varphi &= \frac{1}{2}(K_6 + iK_7), & \varphi^\dagger\varphi &= \frac{K_0}{\sqrt{6}} - \frac{K_8}{\sqrt{3}}. \end{aligned} \quad (27)$$

Further, we decompose the complex singlets into its real and imaginary parts,

$$\sigma = \frac{1}{\sqrt{2}}(\sigma_R + i\sigma_I), \quad \rho = \frac{1}{\sqrt{2}}(\rho_R + i\rho_I), \quad \xi = \frac{1}{\sqrt{2}}(\xi_R + i\xi_I). \quad (28)$$

With the replacements (27) and (28), the potential can be written in terms of the bilinears as well as the real and imaginary parts of the singlets, $V(K_0, \dots, K_8, \sigma_R, \sigma_I, \rho_R, \rho_I, \xi_R, \xi_I, \chi, \zeta)$.

All gauge degrees of freedom are systematically avoided and all fields and parameters are real in this form.

We now look for all stationary points of the potential, in order to find the global minimum, or in the degenerate case, the global minima. For a stable potential, the global minimum is given by the deepest stationary point. We now classify the stationary points with respect to the rank of the matrix \underline{K} . Any stationary point with rank 2 of \underline{K} corresponds to a fully broken electroweak symmetry, rank 0 to an unbroken electroweak symmetry, and rank 1 to a physically acceptable breaking of $SU(2)_L \times U(1)_Y \rightarrow U(1)_{\text{em}}$. The rank conditions result in different sets of polynomial equations. Explicitly, the set of equations corresponding to the rank 2 are,

$$\begin{aligned} \nabla_{K_0, \dots, K_8, \sigma_R, \sigma_I, \rho_R, \rho_I, \xi_R, \xi_I, \chi, \zeta} \left[V(K_0, \dots, K_8, \sigma_R, \sigma_I, \rho_R, \rho_I, \xi_R, \xi_I, \chi, \zeta) - u \det(\underline{K}) \right] &= 0, \\ 2K_0^2 - \sum_{a=1}^8 K_a K_a &> 0, \\ \det(\underline{K}) &= 0, \\ K_0 &> 0. \end{aligned} \quad (29)$$

Here u denotes a Lagrange multiplier.

For the solutions with rank 0 of \underline{K} , we set all bilinears to zero and look for the stationary points of the corresponding potential, that is, solutions of the set of equations,

$$\nabla_{\sigma_R, \sigma_I, \rho_R, \rho_I, \xi_R, \xi_I, \chi, \zeta} V(K_0 = 0, \dots, K_8 = 0, \sigma_R, \sigma_I, \rho_R, \rho_I, \xi_R, \xi_I, \chi, \zeta) = 0. \quad (30)$$

With respect to rank 1 solutions of \underline{K} , we can parametrize the matrix \underline{K} in terms of the three-component complex vector $w = (w_1, w_2, w_3)^T$,

$$\underline{K} = K_0 \sqrt{\frac{3}{2}} \mathbf{w} \mathbf{w}^\dagger, \quad (31)$$

getting for the bilinears

$$K_\alpha(K_0, \mathbf{w}^\dagger, \mathbf{w}) = K_0 \sqrt{\frac{3}{2}} \mathbf{w}^\dagger \lambda_\alpha \mathbf{w}, \quad \alpha = 0, \dots, 8. \quad (32)$$

The potential can now be written as $V(K_0, \mathbf{w}^\dagger, \mathbf{w}, \sigma_R, \sigma_I, \rho_R, \rho_I, \xi_R, \xi_I, \chi, \zeta)$ and the corresponding set of polynomial equations reads

$$\begin{aligned} \nabla_{K_0, w_1, w_2, w_3, \sigma_R, \sigma_I, \rho_R, \rho_I, \xi_R, \xi_I, \chi, \zeta} [V(K_0, \mathbf{w}^\dagger, \mathbf{w}, \sigma_R, \sigma_I, \rho_R, \rho_I, \xi_R, \xi_I, \chi, \zeta) - u(\mathbf{w}^\dagger \mathbf{w} - 1)] &= 0, \\ \mathbf{w}^\dagger \mathbf{w} - 1 &= 0, \\ K_0 &> 0, \end{aligned} \quad (33)$$

where u again denotes a Lagrange multiplier. We solve the three sets of equations (29), (30), (33) and the solution with the lowest potential value is (are) the global minimum (minima). A solution is only physically acceptable if it originates from the set (33), corresponding to the observed electroweak symmetry-breaking. In addition, we have to check that the vacuum gives the observed VEV v . Numerically, we accept solutions which provide a vacuum-expectation value in the range $245 \text{ GeV} < v < 247 \text{ GeV}$. The sets of equations can be solved via homotopy continuation; see for instance [163]. The homotopy continuation algorithms can be found implemented in the open-source software package PHCpack [164]. We have numerically checked that there is large parameter space available fulfilling the stationarity and stability conditions of the potential. Also the potential can provide sufficiently heavy scalars, apart from the SM-like Higgs boson, in accordance with the experimental constraints.

IV. THE HIGGS MASS SPECTRUM

Here we restrict ourselves to real parameters of the potential (18), that is, in particular we consider a CP conserving scalar sector. Then, we find that the spectrum of the physical CP even neutral scalars is composed of the 126 GeV SM-like Higgs boson, i.e h , two heavy CP even scalars H_1 and H_2 as well as the inert scalars transforming non-trivially under the $Z_2^{(2)}$ symmetry and (or) having complex Z_4 charges, namely $\varphi_R^0, \rho_R, \xi_R, S_1$ and S_2 . For the sake of simplicity, we consider the scenario of the decoupling limit which is motivated by the experimental fact that the couplings of the 126 GeV SM-like Higgs boson are very close to the SM expectation. In the decoupling limit ϕ_R^0 corresponds to the 126 GeV SM-like Higgs boson, i.e h . The squared masses of the $\phi_R^0, \varphi_R^0, \rho_R, \xi_R$ scalars are given by:

$$\begin{aligned} m_h^2 &= 2\lambda_1 v^2, & m_{\varphi_R^0}^2 &= \mu_3^2 + \frac{1}{2}(\lambda_5 + \lambda_8 + \lambda_{11})v^2 + \alpha_{17}v_\chi^2 + \alpha_{18}v_\zeta^2, \\ m_{\rho_R}^2 &= \mu_6^2 + \frac{\alpha_3}{2}v^2 + \kappa_{12}v_\chi^2 + \kappa_{15}v_\zeta^2 + 2\kappa_{17}v_\zeta v_\chi, & m_{\xi_R}^2 &= \mu_7^2 + \frac{\alpha_4}{2}v^2 + \kappa_{13}v_\chi^2 + \kappa_{16}v_\zeta^2 + 2\kappa_{18}v_\zeta v_\chi. \end{aligned} \quad (34)$$

The scalar fields H_1 and H_2 are physical mass eigenstates of the following squared scalar mass matrix written in the $(\tilde{\chi}, \tilde{\zeta})$ basis:

$$M_H^2 = \begin{pmatrix} 8\kappa_4 v_\chi^2 & 4\kappa_{10} v_\chi v_\zeta \\ 4\kappa_{10} v_\chi v_\zeta & 8\kappa_5 v_\zeta^2 \end{pmatrix}, \quad (35)$$

This matrix can be diagonalized as follows:

$$\begin{aligned} R_H^T M_H^2 R_H &= \begin{pmatrix} 4\kappa_4 v_\chi^2 + 4\kappa_5 v_\zeta^2 + 4\sqrt{(\kappa_4 v_\chi^2 - \kappa_5 v_\zeta^2)^2 + \kappa_{10} v_\chi^2 v_\zeta^2} & 0 \\ 0 & 4\kappa_4 v_\chi^2 + 4\kappa_5 v_\zeta^2 - 4\sqrt{(\kappa_4 v_\chi^2 - \kappa_5 v_\zeta^2)^2 + \kappa_{10} v_\chi^2 v_\zeta^2} \end{pmatrix}, \\ R_H &= \begin{pmatrix} \cos \theta_H & -\sin \theta_H \\ \sin \theta_H & \cos \theta_H \end{pmatrix} & \tan 2\theta_H &= \frac{\kappa_{10} v_\chi v_\zeta}{\kappa_4 v_\chi^2 - \kappa_5 v_\zeta^2}. \end{aligned} \quad (36)$$

Consequently, the physical scalar mass eigenstates states of the matrix M_H^2 are given by:

$$\begin{pmatrix} H_1 \\ H_2 \end{pmatrix} = \begin{pmatrix} \cos \theta_H & \sin \theta_H \\ -\sin \theta_H & \cos \theta_H \end{pmatrix} \begin{pmatrix} \tilde{\chi} \\ \tilde{\zeta} \end{pmatrix}. \quad (37)$$

Their squared masses are:

$$m_{H_{1/2}}^2 = 4\kappa_4 v_\chi^2 + 4\kappa_5 v_\zeta^2 \pm 4\sqrt{(\kappa_4 v_\chi^2 - \kappa_5 v_\zeta^2)^2 + \kappa_{10} v_\chi^2 v_\zeta^2}. \quad (38)$$

The scalar fields S_1 and S_2 are physical mass eigenstates of the following squared scalar mass matrix written in the (η_R^0, σ_R) basis:

$$M_H^2 = \begin{pmatrix} \mu_2^2 + \frac{1}{2}(\lambda_4 + \lambda_7 + \lambda_{10})v^2 + \alpha_{15}v_\chi^2 + \alpha_{16}v_\zeta^2 & \frac{1}{\sqrt{2}}Av \\ \frac{1}{\sqrt{2}}Av & \mu_4^2 + 2\mu_5^2 + \frac{1}{2}(\alpha_1 + 2\alpha_2)v^2 + \kappa_{11}v_\chi^2 + \kappa_{14}v_\zeta^2 \end{pmatrix}, \quad (39)$$

This matrix can be diagonalized as follows:

$$\begin{aligned} R_S^T M_S^2 R_S &= \begin{pmatrix} \frac{A_S+B_S}{2} - \frac{1}{2}\sqrt{(A_S-B_S)^2 + 4C_S^2} & 0 \\ 0 & \frac{A_S+B_S}{2} + \frac{1}{2}\sqrt{(A_S-B_S)^2 + 4C_S^2} \end{pmatrix}, \\ R_S &= \begin{pmatrix} \cos \theta_S & -\sin \theta_S \\ \sin \theta_S & \cos \theta_S \end{pmatrix}, \\ A_S &= \mu_2^2 + \frac{1}{2}(\lambda_4 + \lambda_7 + \lambda_{10})v^2 + \alpha_{15}v_\chi^2 + \alpha_{16}v_\zeta^2, & B_S &= \mu_4^2 + 2\mu_5^2 + \frac{1}{2}(\alpha_1 + 2\alpha_2)v^2 + \kappa_{11}v_\chi^2 + \kappa_{14}v_\zeta^2, \\ C_S &= \frac{1}{\sqrt{2}}Av, & \tan 2\theta_S &= \frac{2C_S}{A_S - B_S}. \end{aligned} \quad (40)$$

Consequently, the physical scalar mass eigenstates states of the matrix M_S^2 are given by:

$$\begin{pmatrix} S_1 \\ S_2 \end{pmatrix} = \begin{pmatrix} \cos \theta_S & \sin \theta_S \\ -\sin \theta_S & \cos \theta_S \end{pmatrix} \begin{pmatrix} \eta_R^0 \\ \sigma_R \end{pmatrix}. \quad (41)$$

Their squared masses are:

$$m_{S_{1/2}}^2 = \frac{A_S + B_S}{2} \pm \frac{1}{2}\sqrt{(A_S - B_S)^2 + 4C_S^2}. \quad (42)$$

Concerning the CP odd scalar sector, we find that it is composed of one massless pseudoscalar state, i.e. ϕ_I^0 , which is identified with the neutral SM Nambu-Goldstone boson G_Z^0 eaten up by the longitudinal component of the Z gauge boson, as well as four physical pseudoscalar fields $\varphi_I^0, \rho_I, \xi_I, P_1$ and P_2 . The squared masses of the $\phi_I^0, \varphi_I^0, \rho_I$ scalars are given by:

$$\begin{aligned} m_{\phi_I^0}^2 &= 0, & m_{\varphi_I^0}^2 &= \mu_3^2 + \frac{1}{2}(\lambda_5 + \lambda_8 - \lambda_{11})v^2 + \alpha_{17}v_\chi^2 + \alpha_{18}v_\zeta^2, \\ m_{\rho_I}^2 &= \mu_6^2 + \frac{\alpha_3}{2}v^2 + \kappa_{12}v_\chi^2 + \kappa_{15}v_\zeta^2 - 2\kappa_{17}v_\zeta v_\chi, & m_{\xi_I}^2 &= \mu_7^2 + \frac{\alpha_4}{2}v^2 + \kappa_{13}v_\chi^2 + \kappa_{16}v_\zeta^2 - 2\kappa_{18}v_\zeta v_\chi. \end{aligned} \quad (43)$$

The scalar fields P_1 and P_2 are the physical mass eigenstates of the following squared scalar mass matrix written in the (η_I^0, σ_I) -basis:

$$M_P^2 = \begin{pmatrix} \mu_2^2 + \frac{1}{2}(\lambda_4 + \lambda_7 - \lambda_{10})v^2 + \alpha_{15}v_\chi^2 + \alpha_{16}v_\zeta^2 & -\frac{1}{\sqrt{2}}Av \\ -\frac{1}{\sqrt{2}}Av & \mu_4^2 - 2\mu_5^2 + \frac{1}{2}(\alpha_1 - 2\alpha_2)v^2 + \kappa_{11}v_\chi^2 + \kappa_{14}v_\zeta^2 \end{pmatrix}, \quad (44)$$

which can be diagonalized by the transformation:

$$\begin{aligned}
R_P^T M_P^2 R_P &= \begin{pmatrix} \frac{A_P+B_P}{2} + \frac{1}{2}\sqrt{(A_P-B_P)^2 + 4C_P^2} & 0 \\ 0 & \frac{A_P+B_P}{2} - \frac{1}{2}\sqrt{(A_P-B_P)^2 + 4C_P^2} \end{pmatrix}, \\
R_P &= \begin{pmatrix} \cos \theta_P & -\sin \theta_P \\ \sin \theta_P & \cos \theta_P \end{pmatrix}, \\
A_P &= \mu_2^2 + \frac{1}{2}(\lambda_4 + \lambda_7 - \lambda_{10})v^2 + \alpha_{15}v_\chi^2 + \alpha_{16}v_\zeta^2, & B_P &= \mu_4^2 - 2\mu_5^2 + \frac{1}{2}(\alpha_1 - 2\alpha_2)v^2 + \kappa_{11}v_\chi^2 + \kappa_{14}v_\zeta^2, \\
C_P &= -\frac{1}{\sqrt{2}}Av, & \tan 2\theta_P &= \frac{2C_P}{A_P - B_P}.
\end{aligned} \tag{45}$$

Consequently, the physical scalar mass eigenstates $P_{1,2}$ are given by:

$$\begin{pmatrix} P_1 \\ P_2 \end{pmatrix} = \begin{pmatrix} \cos \theta_P & \sin \theta_P \\ -\sin \theta_P & \cos \theta_P \end{pmatrix} \begin{pmatrix} \eta_I^0 \\ \sigma_I \end{pmatrix}. \tag{46}$$

Their squared masses are:

$$m_{P_1}^2 = \frac{A_P + B_P}{2} + \frac{1}{2}\sqrt{(A_P - B_P)^2 + 4C_P^2}, \quad m_{P_2}^2 = \frac{A_P + B_P}{2} - \frac{1}{2}\sqrt{(A_P - B_P)^2 + 4C_P^2}. \tag{47}$$

In the charged scalar sector we find two massless Nambu-Goldstone states, ϕ^\pm , absorbed by the longitudinal components of W^\pm gauge bosons, as well as four physical charged scalars, η^\pm , φ^\pm with the masses:

$$m_{\eta^\pm}^2 = \mu_2^2 + \frac{1}{2}\lambda_4v^2 + \alpha_{15}v_\chi^2 + \alpha_{16}v_\zeta^2, \quad m_{\varphi^\pm}^2 = \mu_3^2 + \frac{1}{2}\lambda_5v^2 + \alpha_{17}v_\chi^2 + \alpha_{18}v_\zeta^2. \tag{48}$$

This completes the list of the scalar sector of our model.

V. SM FERMION MASS HIERARCHY

The SM fermion mass matrices are generated in our model according to the diagrams in Fig. 1, with the Yukawa interactions in (14)-(17). We write the mass matrices for the charged fermions in the form

$$M_U = \begin{pmatrix} \left(\begin{array}{ccc} (a_{11}^{(u)})^3 l^2 & (a_{12}^{(u)})^2 l & a_{13}^{(u)} \\ (a_{21}^{(u)})^3 l^2 & (a_{22}^{(u)})^2 l & a_{23}^{(u)} \\ (a_{31}^{(u)})^3 l^2 & (a_{32}^{(u)})^2 l & a_{33}^{(u)} \end{array} \right) \frac{v}{\sqrt{2}}, & M_D = \begin{pmatrix} \left(\begin{array}{ccc} (a_{11}^{(d)})^3 l^2 & (a_{12}^{(d)})^2 l^2 & (a_{13}^{(d)})^2 l \\ (a_{21}^{(d)})^3 l^2 & (a_{22}^{(d)})^2 l^2 & (a_{23}^{(d)})^2 l \\ (a_{31}^{(d)})^3 l^2 & (a_{32}^{(d)})^2 l^2 & (a_{33}^{(d)})^2 l \end{array} \right) \frac{v}{\sqrt{2}} \end{pmatrix} \tag{49}$$

$$M_l = \begin{pmatrix} \left(\begin{array}{ccc} (a_{11}^{(l)})^3 l^2 & (a_{12}^{(l)})^2 l & (a_{13}^{(l)})^2 l \\ (a_{21}^{(l)})^3 l^2 & (a_{22}^{(l)})^2 l & (a_{23}^{(l)})^2 l \\ (a_{31}^{(l)})^3 l^2 & (a_{32}^{(l)})^2 l & (a_{33}^{(l)})^2 l \end{array} \right) \frac{v}{\sqrt{2}} \end{pmatrix} \tag{50}$$

Here we have taken into account the loop level at which the columns of these matrices are generated, in particular $l \approx (1/4\pi)^2$ is the loop suppression factor.

The powers of this loop factor in (49), (50), explicitly display the following picture that we have in our model: The third column in M_U is generated at the tree-level, engendering mass to the top quark. The second and first columns of M_U arise at the one and two-loop levels, respectively, and are associated with the charm and up quark masses. The light down and strange quark masses are also generated at two-loop level. On the other hand, the third column of M_D arise at one-loop level.

As for the SM charged lepton mass matrix M_l , its first column, responsible for the electron mass, appears at the two-loop level, whereas its second and third columns, providing masses to the muon and the tau lepton, respectively, are generated at one loop.

As we pointed out before, the objective of the model is to generate the observed hierarchy of the fermion mass spectrum in terms of loop suppression. Therefore, it is crucial that the quark masses and mixings predicted by the model are reproduced with parameters $a_{ij}^{(u)}, a_{ij}^{(d)} \sim \mathcal{O}(1)$ ($i, j = 1, 2, 3$). Let us check this essential point in detail: We use the experimental values of the quark masses [165], the CKM parameters [166] and the charged lepton masses [166]:

$$\begin{aligned}
m_u(\text{MeV}) &= 1.24 \pm 0.22, & m_d(\text{MeV}) &= 2.69 \pm 0.19, & m_s(\text{MeV}) &= 53.5 \pm 4.6, \\
m_c(\text{GeV}) &= 0.63 \pm 0.02, & m_t(\text{GeV}) &= 172.9 \pm 0.4, & m_b(\text{GeV}) &= 2.86 \pm 0.03, \\
\sin \theta_{12} &= 0.2245 \pm 0.00044, & \sin \theta_{23} &= 0.0421 \pm 0.00076, & \sin \theta_{13} &= 0.00365 \pm 0.00012, \\
J &= (3.18 \pm 0.15) \times 10^{-5}, \\
m_e(\text{MeV}) &= 0.4883266 \pm 0.0000017, & m_\mu(\text{MeV}) &= 102.87267 \pm 0.00021, & m_\tau(\text{MeV}) &= 1747.43 \pm 0.12,
\end{aligned} \tag{51}$$

where, J is the Jarlskog parameter.

By solving the eigenvalue problem for the mass matrices (49), (50) we find a solution for the parameters that reproduces the values in Eq. (51). It is given by

$$a_{ij}^{(u)} = \begin{pmatrix} -0.688435 & 0.23427 & 0.574417 \\ -0.433888 & 0.975784 & 0.575768 \\ 0.460125 & 0.299329 & 0.572606 \end{pmatrix}, \tag{52}$$

$$a_{ij}^{(d)} = \begin{pmatrix} 0.496199 - 0.856786i & 0.553843 - 0.956252i & 0.988976 + 0.00132749i \\ 0.0000811073 - 0.9244i & 0.000107414 - 1.13112i & 0.924773 + 0.0000767587i \\ 0.00207731 + 0.985775i & 0.00249437 + 1.15427i & 0.987132 - 0.00207885i \end{pmatrix}, \tag{53}$$

$$a_{ij}^{(l)} = \begin{pmatrix} -0.598992 - 0.00493263i & 0.00393775 - 0.916528i & 0.77355 + 0.00318633i \\ 0.000405292 + 0.675959i & 0.000325396 + 0.880957i & 0.676159 - 0.000407163i \\ 0.00295785 + 0.801275i & 0.0036143 + 0.898469i & 0.801517 - 0.0029589i \end{pmatrix}.$$

As we can see, all the entries (the absolute values) of the above matrices are of order unity with rather mild deviations. This demonstrates that the proposed model is able to explain the existing pattern of the observed quark spectrum via the sequential loop suppression mechanism.

Finally, the small masses of the active neutrinos are generated at the three-loop level, as follows from the last diagram of Figure 1. Thus, for the neutrino mass matrix we can write

$$M_\nu = l^3 y^6 \lambda \frac{v^2}{M}, \tag{54}$$

with M denoting a common mass scale of the virtual scalars and fermions running in the internal lines of the neutrino loop diagram in Figure 1, y is a matrix of the neutrino Yukawa couplings and λ is the quartic scalar coupling. Using $M \sim \mathcal{O}(13)$ TeV, $y \sim 0.3\mathbb{1}$, and $\lambda \sim 0.1$ in Eq. (54) we find $m_\nu \sim \mathcal{O}(0.1)$ eV, thus showing that the model naturally explains the smallness of the light active neutrino masses with respect to the EWSB scale. Furthermore, from this estimate of the light neutrino masses it is to expect that exotic scalars and fermions beyond the SM should have masses of $\mathcal{O}(13)$ TeV.

VI. CHARGED LEPTON-FLAVOR VIOLATION CONSTRAINTS

In this section we will derive constraints from the non-observation of the charged Lepton Flavor Violating (LFV) process $\mu \rightarrow e\gamma$. The dominant contribution to the decay $l_i \rightarrow l_j\gamma$ occurs in our model at one-loop level and, according to the diagram in Figure 2, is mediated by a virtual electrically charged scalar φ^+ , originating from the $SU(2)_L$ inert doublet φ , and by the right-handed Majorana neutrinos ν_{sR} ($s = 1, 2$). There is also a contribution arising from the charged exotic leptons E_2 and the electrically neutral scalars S_k, P_k . However this contribution is sub-leading since it only appears at the two loop level, as shown in Appendix A. Therefore, we can safely neglect it.

Then we find for the branching ratio corresponding to the diagram in Fig. 2 the following expression [167–170]

$$Br(l_i \rightarrow l_j \gamma) = \frac{3(4\pi)^3 \alpha_{em}}{4G_F^2} \left| \sum_{s=1}^2 \frac{x_{is}^{(\nu)} x_{js}^{(\nu)}}{2(4\pi)^2 m_{\varphi^\pm}^2} F\left(\frac{m_{\nu_{sR}}^2}{m_{\varphi^\pm}^2}\right) \right|^2 Br(l_i \rightarrow l_j \nu_i \bar{\nu}_j),$$

$$F(x) = \frac{1 - 6x + 3x^2 + 2x^3 - 6x^2 \ln x}{6(1-x)^4}. \quad (55)$$

Here $x_{is}^{(\nu)} = \sum_{k=1}^3 y_{ks}^{(\nu)} (V_{lL}^\dagger)_{ik}$ and m_{φ^\pm} are the masses of the charged scalar components of the $SU(2)_L$ inert doublet φ , whereas $m_{\nu_{sR}}$ ($s = 1, 2$) correspond to the masses of the right-handed Majorana neutrinos ν_{sR} . To simplify our anal-

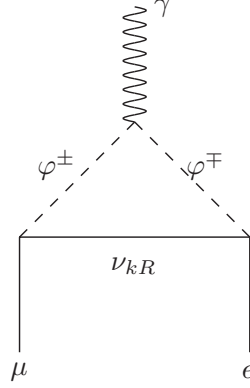


Figure 2: Feynman diagram corresponding to the dominant contribution to the $\mu \rightarrow e\gamma$ decay.

ysis we choose a benchmark scenario where the right-handed Majorana neutrinos ν_{sR} are all degenerate with respect to a common mass m_N . In our numerical analysis we vary these masses in the following ranges $1 \text{ TeV} \leq m_{\varphi^\pm} \leq 30 \text{ TeV}$ and $10 \text{ MeV} \lesssim m_N \leq 100 \text{ MeV}$. We also vary the dimensionless couplings in the window $0.1 \leq x_{is}^{(\nu)} \leq 1$ ($i = 1, 2, 3$ and $s = 1, 2$). Let us note that we scanned only over the MeV scale masses for the right-handed Majorana neutrinos ν_{sR} , since these masses are generated at the two-loop level, as seen from the two-loop sub-diagram of the third Feynman diagram of Fig. 1. This is the same loop level at which masses of light and strange quarks, lying in the MeV region, are generated. The results of our analysis are displayed in Figures 3 and 4. In Figure 3 we plot the allowed parameter space in the $m_{\varphi^\pm} - x_{js}^{(\nu)}$ plane consistent with the existing $\mu \rightarrow e\gamma$ experimental constraints. This plot is obtained by randomly generating the parameters m_N , m_{φ^\pm} , $x_{is}^{(\nu)}$ and $x_{js}^{(\nu)}$ in a range of values where the $\mu \rightarrow e\gamma$ branching ratio is below its upper experimental limit of 4.2×10^{-13} [170]. As can be seen from Figure 3, this condition is satisfied for the charged scalar masses m_{φ^\pm} larger than about 3.5 TeV. We also find that in the same region of parameter space, our model predicts branching ratios for the $\tau \rightarrow \mu\gamma$ and $\tau \rightarrow e\gamma$ decays up to 10^{-10} , which is below their corresponding upper experimental bounds of 4.4×10^{-9} and 3.3×10^{-9} , respectively. Consequently, the model is compatible with the current charged lepton-flavor-violating decay constraints. The branching ratio for the $\mu \rightarrow e\gamma$ decay as a function of the charged scalar mass m_{φ^\pm} is shown in Fig. 4 for different values of the $x_{js}^{(\nu)}$ couplings. This Figure shows that the branching ratio for the $\mu \rightarrow e\gamma$ decay decreases as the charged scalar masses m_{φ^\pm} acquire larger values. The horizontal line corresponds to the experimental upper bound of 4.2×10^{-13} [170] for the branching ratio of the $\mu \rightarrow e\gamma$ decay. Here we set $m_N = 50 \text{ MeV}$. We have checked that the branching ratio for the $\mu \rightarrow e\gamma$ decay has a very low sensitivity to the mass m_N of the right-handed Majorana neutrinos ν_{sR} ($s = 1, 2$).

Given that future experiments, such as Mu2e and COMET [171], are expected to measure or at least constrain lepton-flavor conversion in nuclei with much better precision than the radiative lepton LFV decays, we proceed to derive constraints imposed on the model parameter space by $\mu - e$ conversion in nuclei. The $\mu^- - e^-$ conversion ratio is defined [170] as:

$$\text{CR}(\mu - e) = \frac{\Gamma(\mu^- + \text{Nucleus}(A, Z) \rightarrow e^- + \text{Nucleus}(A, Z))}{\Gamma(\mu^- + \text{Nucleus}(A, Z) \rightarrow \nu_\mu + \text{Nucleus}(A, Z - 1))} \quad (56)$$

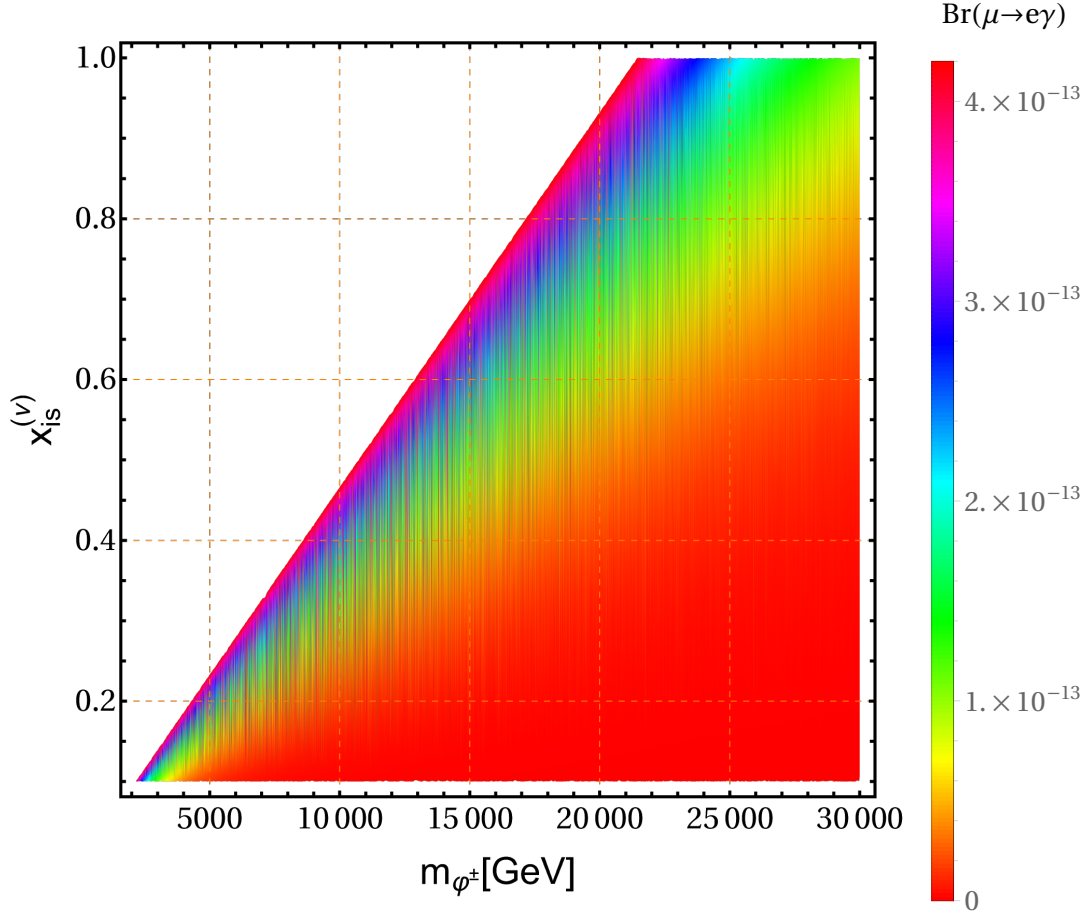


Figure 3: Allowed parameter space in the $m_{\phi^\pm} - x_{j_s}^{(\nu)}$ plane consistent with the charged lepton flavor-violating constraints.

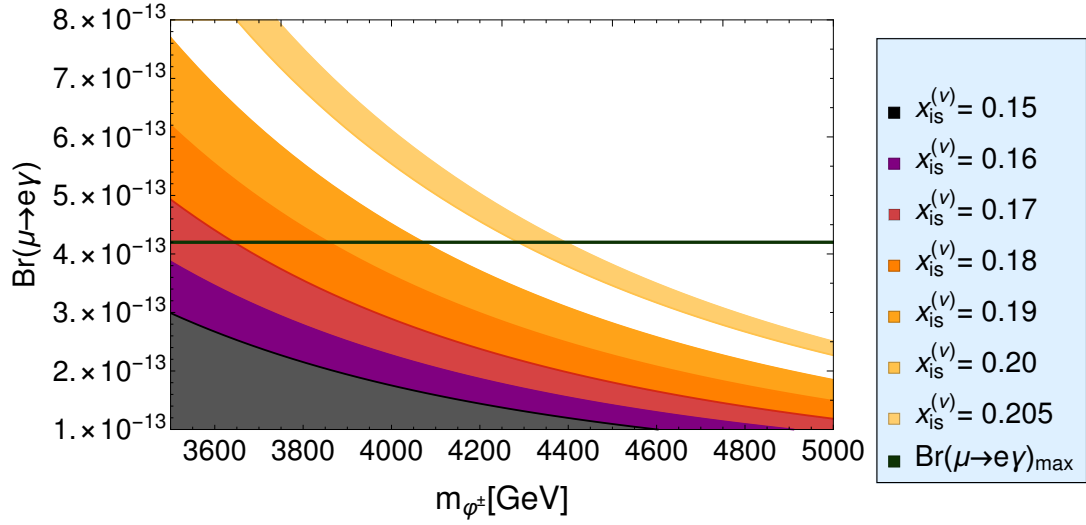


Figure 4: Branching ratio for the $\mu \rightarrow e\gamma$ decay as function of charged scalar masses m_{ϕ^\pm} for different values of the $x_{j_s}^{(\nu)}$ couplings. The horizontal line corresponds to the experimental upper bound of 4.2×10^{-13} [170] for the branching ratio of the $\mu \rightarrow e\gamma$ decay. Here we have set $m_N = 50$ MeV

Using an Effective Lagrangian approach for describing LFV processes, as done in [172], and considering the low momentum limit, where the off-shell contributions from photon exchange are negligible with respect to the contributions arising from real photon emission, the dipole operators shown in Ref. [172] dominate the conversion rate, thus, yielding the following relations [170, 172]:

$$\text{CR}(\mu\text{Ti} \rightarrow e\text{Ti}) \simeq \frac{1}{200} \text{Br}(\mu \rightarrow e\gamma) \quad \text{CR}(\mu\text{Al} \rightarrow e\text{Al}) \simeq \frac{1}{350} \text{Br}(\mu \rightarrow e\gamma) \quad (57)$$

Notice that the aforementioned relations are valid for the case of photon dominance in the $\mu^- - e^-$ conversion, which applies to our model due to the absence of tree-level flavor changing neutral scalar interactions. Therefore, experimental upper bounds on the conversion rates (56) will translate in our model to upper limits on $\text{Br}(\mu \rightarrow e\gamma)$.

The sensitivity of the CERN Neutrino Factory, which will use a Titanium target [173], is expected at the level of $\sim 10^{-18}$. The expected sensitivities of the next generation experiments such as Mu2e and COMET [171], with an Aluminum target, are expected to be about $\sim 10^{-17}$. Thus, according to Eqs. (57), the future limits will result in about three order of magnitude improvement in $\text{Br}(\mu \rightarrow e\gamma)$.

In Figure 5 we show the $\text{CR}(\mu\text{Ti} \rightarrow e\text{Ti})$ (top plot) and $\text{CR}(\mu\text{Al} \rightarrow e\text{Al})$ (bottom plot), as function of the charged scalar mass m_{φ^\pm} for different values of the dimensionless couplings $x_{js}^{(\nu)}$ ($j = 1, 2, 3$, $n = 1, 2$). The black horizontal lines correspond to the expected sensitivities $\sim 10^{-18}$ (top plot) of the CERN Neutrino Factory [173] and $\sim 10^{-17}$ (bottom plot) of the next generation of experiments such as Mu2e and COMET [171]. In these plots we have set $m_N = 50$ MeV. The plots show that the next generation experiments, where titanium and aluminium will be used as targets, can rule out the part of the model parameter space where the charged scalar masses are lower than about 10 TeV for $x_{js}^{(\nu)} \simeq \mathcal{O}(0.1)$.

VII. MUON AND ELECTRON ANOMALOUS MAGNETIC MOMENT.

The results of the experimental measurements of the anomalous magnetic dipole moments of electron and muon $a_{e,\mu} = (g_{e,\mu} - 2)/2$ show significant deviation from their SM values

$$\Delta a_\mu = a_\mu^{\text{exp}} - a_\mu^{\text{SM}} = (2.51 \pm 0.59) \times 10^{-9} \quad [56, 154, 174-179] \quad (58)$$

$$\Delta a_e = a_e^{\text{exp}} - a_e^{\text{SM}} = (-0.88 \pm 0.36) \times 10^{-12} \quad [180], \quad (4.8 \pm 3.0) \times 10^{-13} \quad [181] \quad (59)$$

Here the value of a_μ^{exp} is a combined result of the BNL E821 experiment [182] and the recently announced FNAL Muon g-2 measurement [154], showing the 4.2σ tension between the SM and experiment. The last positive value for Δa_e corresponds to the recently published new measurement of the fine-structure constant with an accuracy of 81 parts per trillion [181]. In this section we analyze predictions of our model for these observables. The leading contributions to $\Delta a_{e,\mu}$ arising in the model are shown in Figs. 6, 7.

For simplicity we set $\theta_S = \theta_P = \theta$ and $y_{22}^{(l)} = x_{22}^{(l)} = y_{21}^{(\nu)} = y_{22}^{(\nu)} = y$ (for the definitions see Eqs. (16), (17), (40) and (45)). Furthermore, we work on a simplified benchmark scenario with a diagonal SM charged lepton mass matrix, where the charged exotic leptons $\tilde{E}, \tilde{E}'; E_1$ and E_2 , only contribute to the electron, muon and tau masses, respectively. Then, the contribution to the muon anomalous magnetic moment takes the form

$$\begin{aligned} \Delta a_\mu = & \frac{y^2 m_\mu^2}{8\pi^2} [I_S(m_{E_1}, m_{S_1}) - I_S(m_{E_1}, m_{S_2}) + I_P(m_{E_1}, m_{P_1}) - I_P(m_{E_1}, m_{P_2})] \sin\theta \cos\theta \\ & - \frac{y_2^2 m_\mu^2}{16\pi^2 m_{\varphi^\pm}^2} \sum_{s=1}^2 F\left(\frac{m_{\nu_{sR}}^2}{m_{\varphi^\pm}^2}\right), \end{aligned} \quad (60)$$

where the loop integral $F(x)$ is defined in Eq. (55) and was previously computed in Ref. [167], whereas $I_{S(P)}(m_E, m)$ has the form [170, 183-186]

$$I_{S(P)}(m_E, m) = \int_0^1 \frac{x^2 \left(1 - x \pm \frac{m_E}{m_\mu}\right)}{m_\mu^2 x^2 + (m_E^2 - m_\mu^2)x + m^2(1-x)} dx. \quad (61)$$

In our numerical analysis we consider a benchmark scenario with $\theta = \frac{\pi}{4}$, $m_{\nu_{1R}} = m_{\nu_{2R}} = 50$ MeV, $M_{P_1} = M_{S_1} = 0.5$ TeV, $M_{P_2} = 0.6$ TeV, $M_{S_2} = 1$ TeV and $m_{\varphi^+} = 4$ TeV. The mass of the charged exotic lepton E_1 has been varied

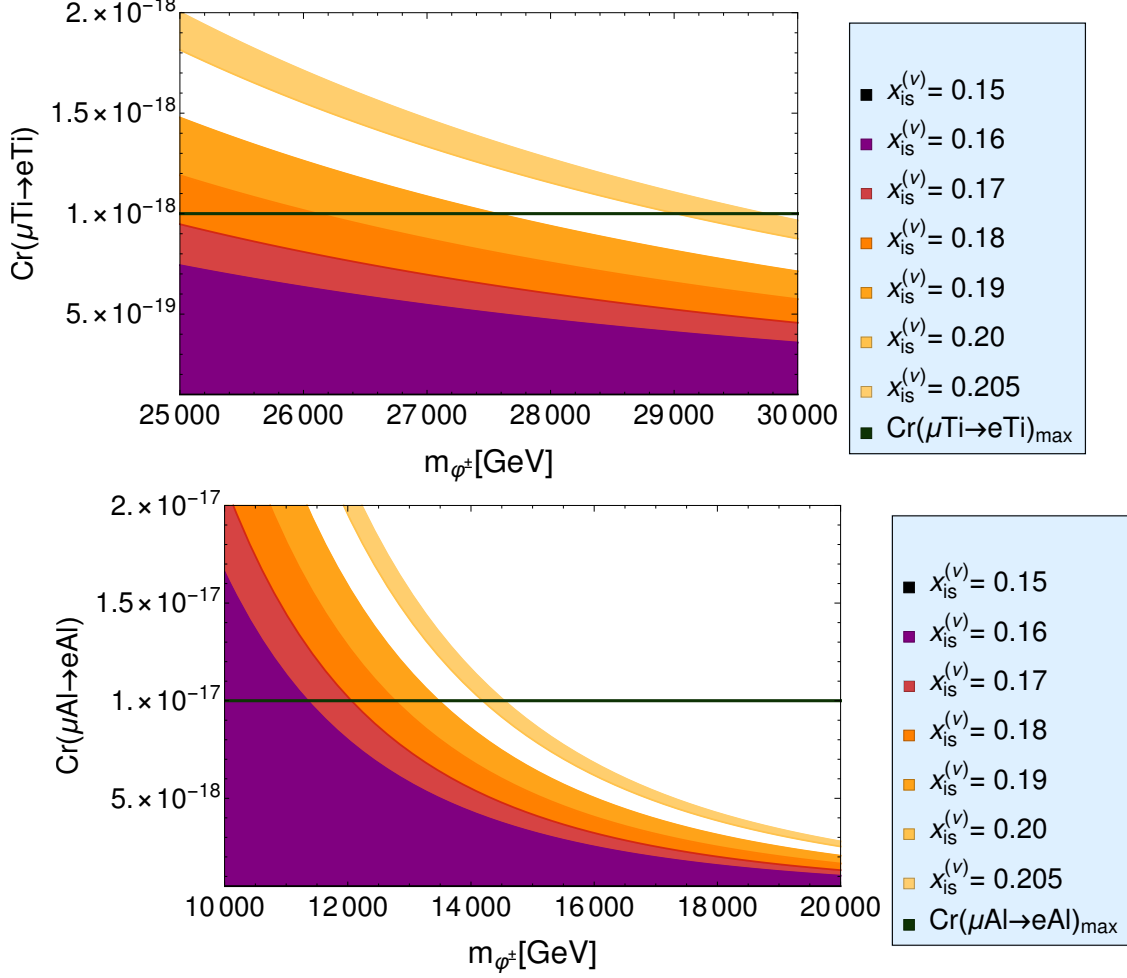


Figure 5: $CR(\mu\text{Ti} \rightarrow e\text{Ti})$ (top plot) and $CR(\mu\text{Al} \rightarrow e\text{Al})$ (bottom plot) as function of the charged scalar masses m_{φ^\pm} , for different values of the $x_{js}^{(\nu)}$ couplings ($j = 1, 2, 3$, $n = 1, 2$). The black horizontal line in each plot corresponds to the expected sensitivities of the next generation of experiments that will use titanium [173] and aluminum [171] as targets, respectively. Here we have set $m_N = 50$ MeV.

in the ranges $6 \text{ TeV} \leq M_{E_1} \leq 8 \text{ TeV}$. Note that these masses for the right-handed Majorana neutrinos ν_{sR} ($s = 1, 2$) and for the electrically charged scalar φ^+ are consistent with the constraints arising from the charged lepton flavor processes $\mu \rightarrow e\gamma$, $\tau \rightarrow \mu\gamma$ and $\tau \rightarrow e\gamma$, as shown in the previous section. Considering that the muon anomalous magnetic moment is constrained to be in the range shown in (58), we plot in Fig. 8 the muon anomalous magnetic moment as a function of the charged exotic lepton mass M_{E_1} . Figure 8 shows that the muon anomalous magnetic moment decreases when the charged exotic lepton mass is increased.

The anomalous magnetic moment of the electron Δa_e can be computed in an analogous way as Δa_μ . The difference is that the neutral (pseudo-)scalars and exotic charged leptons contribution to the Δa_e appears at two-loop level, as shown in Appendix A, and is therefore sub-leading. Thus, Δa_e is dominated by the effective vertex diagram in Fig 7, involving the electrically charged scalar φ^+ , which couples to the right-handed Majorana neutrinos ν_{sR} ($s = 1, 2$). From this diagram we find in an approximate form [167]

$$\Delta a_e \approx -\frac{y_1^2 m_e^2}{16\pi^2 m_{\varphi^\pm}^2} \sum_{s=1}^2 F\left(\frac{m_{\nu_{sR}}^2}{m_{\varphi^\pm}^2}\right). \quad (62)$$

Consequently, our model predicts negative values for this observable in accordance with [180]. However, in order to reproduce either [180] or [181], the experimental values shown in (59), we need that the mass of the electrically charged scalar φ^\pm lies in the interval $100 \text{ GeV} \lesssim m_{\varphi^\pm} \lesssim 150 \text{ GeV}$. These values are incompatible with the $\mu \rightarrow e\gamma$ constraints analyzed in Section VI. The latter require $m_{\varphi^\pm} \geq 3.5 \text{ TeV}$, which will yield in this case a bit too small

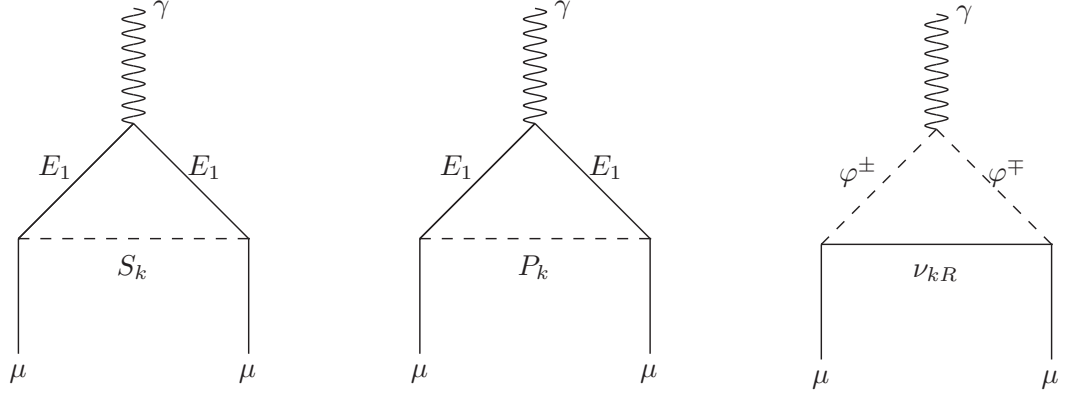


Figure 6: Feynman-loop diagrams contributing to the muon anomalous magnetic moment. Here $k = 1, 2$.

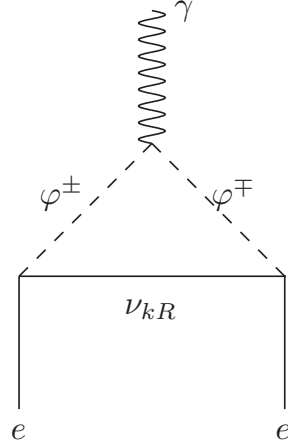


Figure 7: Leading Feynman-loop diagram contributing to the electron anomalous magnetic moment. Here $k = 1, 2$.

value for the electron anomalous magnetic moment, which nonetheless are consistent with the above mentioned 2σ experimentally allowed range.

VIII. DARK MATTER RELIC DENSITY

In this section we provide a discussion of our model in view of Dark Matter (DM). We do not intend to provide a sophisticated analysis of the DM constraints, which is beyond the scope of the present paper. Note that due to the preserved $Z_2^{(2)}$ discrete symmetry and to the residual Z_2 symmetry (arising from the spontaneous breaking of the Z_4 subgroup), our model has several stable scalar DM candidates. As follows from the scalar assignments to the $Z_2^{(2)} \times Z_4$ symmetry, given by Eq. (12), we can assign this role to any of the following scalar particles: φ_R^0 , ρ_R , ξ_R , S_1 , S_2 , φ_I^0 , ρ_I , ξ_I , P_1 or P_2 . Furthermore, our model has a fermionic dark matter candidate, which can be the lightest among the two right-handed Majorana neutrinos ν_{sR} ($s = 1, 2$), since in our model they are the only right-handed Majorana

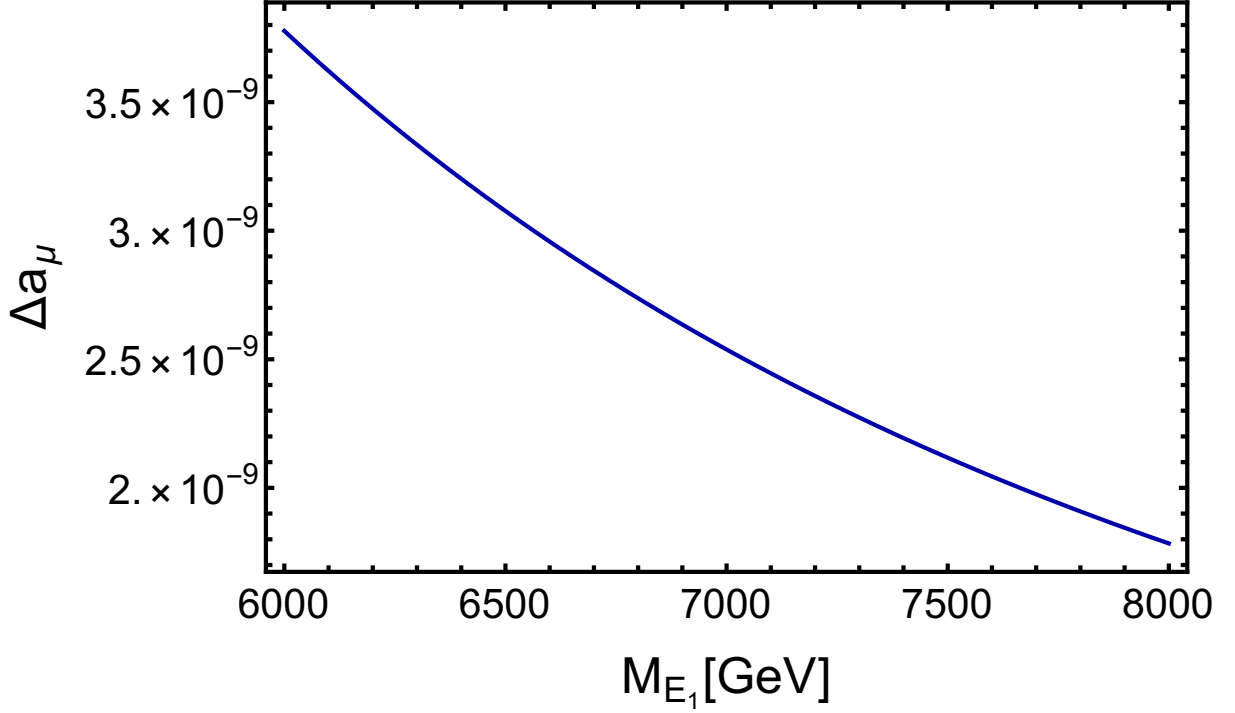


Figure 8: Muon anomalous magnetic moment as a function of the charged exotic lepton mass M_{E_2} .

neutrinos whose masses appear at two-loop level.

Based on Eqs. (34) and (43) of Section III, we take ρ_I as our scalar Dark Matter candidate. To guarantee the stability of ρ_I , we assume that this field is lighter than the charged exotic fermions, and in this way its decay modes into exotic and SM charged fermions are kinematically forbidden.

The relic density of the Dark Matter in the present Universe is estimated as follows (c.f. Ref. [166, 187])

$$\Omega h^2 = \frac{0.1 \text{ pb}}{\langle \sigma v \rangle}, \quad \langle \sigma v \rangle = \frac{A}{n_{eq}^2}, \quad (63)$$

where $\langle \sigma v \rangle$ is the thermally averaged annihilation cross section, A is the total annihilation rate per unit volume at temperature T and n_{eq} is the equilibrium value of the particle density, which are given in [187]

$$A = \frac{T}{32\pi^4} \int_{4m_\phi^2}^{\infty} \sum_{p=W,Z,t,b,h} g_p^2 \frac{s\sqrt{s-4m_{\rho_I}^2}}{2} v_{rel} \sigma(\rho_I \rho_I \rightarrow p\bar{p}) K_1\left(\frac{\sqrt{s}}{T}\right) ds, \\ n_{eq} = \frac{T}{2\pi^2} \sum_{p=W,Z,t,b,h} g_p m_{\rho_I}^2 K_2\left(\frac{m_{\rho_I}}{T}\right), \quad (64)$$

with K_1 and K_2 being the modified Bessel functions of the second kind of order 1 and 2, respectively [187]. For the relic density calculation, we take $T = m_{\rho_I}/20$ as in Ref. [187], which corresponds to a typical freeze-out temperature. The scalar DM candidate ρ_I annihilates mainly into WW , ZZ , $t\bar{t}$, $b\bar{b}$ and hh , via a Higgs portal scalar interaction

$(\phi^\dagger\phi)\rho_I\rho_I$, where ϕ is the SM Higgs doublet. The corresponding annihilation cross sections are given by: [188]:

$$\begin{aligned}
v_{rel}\sigma(\rho_I\rho_I \rightarrow WW) &= \frac{\alpha_3}{32\pi} \frac{s \left(1 + \frac{12m_W^4}{s^2} - \frac{4m_W^2}{s}\right)}{(s - m_h^2)^2 + m_h^2\Gamma_h^2} \sqrt{1 - \frac{4m_W^2}{s}}, \\
v_{rel}\sigma(\rho_I\rho_I \rightarrow ZZ) &= \frac{\alpha_3}{64\pi} \frac{s \left(1 + \frac{12m_Z^4}{s^2} - \frac{4m_Z^2}{s}\right)}{(s - m_h^2)^2 + m_h^2\Gamma_h^2} \sqrt{1 - \frac{4m_Z^2}{s}}, \\
v_{rel}\sigma(\rho_I\rho_I \rightarrow q\bar{q}) &= \frac{N_c\alpha_3^2 m_q^2}{16\pi} \frac{\sqrt{\left(1 - \frac{4m_q^2}{s}\right)^3}}{(s - m_h^2)^2 + m_h^2\Gamma_h^2}, \\
v_{rel}\sigma(\rho_I\rho_I \rightarrow hh) &= \frac{\alpha_3^2}{64\pi s} \left(1 + \frac{3m_h^2}{s - m_h^2} - \frac{2\alpha_3 v^2}{s - 2m_h^2}\right)^2 \sqrt{1 - \frac{4m_h^2}{s}}, \tag{65}
\end{aligned}$$

where \sqrt{s} is the centre-of-mass energy, $N_c = 3$ is the color factor, $m_h = 125.7$ GeV and $\Gamma_h = 4.1$ MeV are the SM Higgs boson h mass and its total decay width, respectively; α_3 is the quartic scalar coupling corresponding to the interaction $\alpha_3(\phi^\dagger\phi)(\rho^\dagger\rho)$.

Fig. 9 displays the relic density Ωh^2 as a function of the mass m_{ρ_I} of the scalar field ρ_I , for several values of the quartic scalar coupling α_3 . The curves from top to bottom correspond to $\alpha_3 = 1, 1.2$ and 1.5 , respectively. The horizontal line corresponds to the experimental value $\Omega h^2 = 0.1198$ of the relic density. Figure 9 shows that the relic density is an increasing function of the mass m_{ρ_I} and a decreasing function of the quartic scalar coupling α_3 . Consequently, an increase in the mass m_{ρ_I} of the scalar field ρ_I will require a larger quartic scalar coupling α_3 , in order to account for the measured value of the Dark Matter relic density, as indicated in Fig. 10.

It is worth mentioning that the Dark Matter relic density constraint yields a linear correlation between the quartic scalar coupling α_3 and the mass m_{ρ_I} of the scalar Dark Matter candidate ρ_I , as shown in Fig. 10. We have numerically checked that in order to reproduce the observed value, $\Omega h^2 = 0.1198 \pm 0.0026$ [189], of the relic density, the mass m_{ρ_I} of the scalar field ρ_I has to be in the range $400 \text{ GeV} \leq m_{\rho_I} \leq 800 \text{ GeV}$, for a quartic scalar coupling α_3 in the range $1 \leq \alpha_3 \leq 1.5$.

In what concerns prospects for the direct DM detection, the scalar DM candidate would scatter off a nuclear target in a detector via Higgs boson exchange in the t -channel, giving rise to a constraint on the coupling of the $(\phi^\dagger\phi)\rho_I\rho_I$ interaction.

IX. CONCLUSIONS

We have constructed an extension of the 3HDM based on the $Z_2^{(1)} \times Z_2^{(2)} \times Z_4$ symmetry, where the SM particle content is enlarged by two inert SU_{2L} scalar doublets, three inert and two active electrically neutral gauge singlet scalars, charged vector like fermions and Majorana neutrinos. These fields are introduced in order to generate the SM fermion mass hierarchy from a sequential loop suppression mechanism: tree-level top quark mass; 1-loop bottom, charm, tau and muon masses; 2-loop masses for the light up, down and strange quarks as well as for the electron; and 3-loop masses for the light active neutrinos. In our model, the $Z_2^{(2)}$ symmetry is preserved, whereas the $Z_2^{(1)}$ symmetry is completely broken and the Z_4 symmetry is broken down to a conserved Z_2 symmetry, thus allowing the stability of the Dark Matter as well as a successful implementation of the aforementioned sequential loop suppression mechanism, without the inclusion of soft symmetry breaking terms. For studying the electroweak symmetry breaking in our model we applied the bilinear formalism of the 3HDM.

We demonstrated that our model successfully accommodates the current fermion mass spectrum and fermionic mixing parameters, the electron and muon anomalous magnetic moments, as well as the constraints arising from charged lepton flavor violating processes.

We have also shown that in our model the branching ratios of the decays $\mu \rightarrow e\gamma$, $\tau \rightarrow \mu\gamma$ and $\tau \rightarrow e\gamma$ can reach values of the order of 10^{-13} , which is within the reach of the future experimental sensitivity, thus making our model testable by the forthcoming experiments.

Finally, we have examined the scalar DM particle candidate of the model and have shown that the prediction is compatible with the observed DM relic density abundance for scalar masses in the range $400 \text{ GeV} \leq m_{\rho_I} \leq 800 \text{ GeV}$.

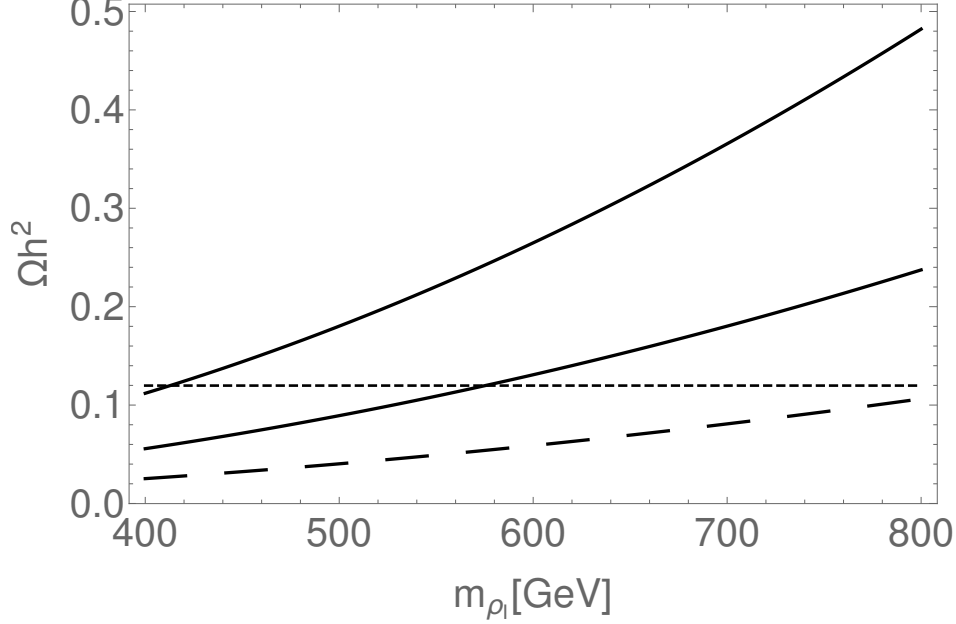


Figure 9: Relic density Ωh^2 , as a function of the mass m_{ρ_I} of the ρ_I scalar field, for several values of the quartic scalar coupling α_3 . The curves from top to bottom correspond to $\alpha_3 = 1, 1.2, 1.5$, respectively. The horizontal line shows the observed value $\Omega h^2 = 0.1198$ [189] for the relic density.

Acknowledgments

A.E.C.H, S.K., M.M, and I.S. are supported by ANID-Chile FONDECYT 1210378, ANID-Chile FONDECYT 1190845, ANID-Chile FONDECYT 1200641, ANID-Chile FONDECYT 1180232, ANID-Chile FONDECYT 3150472, ANID PIA/APOYO AFB180002 and Milenio-ANID-ICN2019.044.

Appendix A: Exotic Leptons and Neutral scalar contribution to Leptonic LFV decays

Let us show that the contribution to $l_i \rightarrow l_j \gamma$ decay of the charged exotic leptons E_2 and the electrically neutral scalars S_k, P_k vanishes at one loop. Their one-loop contribution is given by the first two diagrams in Fig. 6, with one μ replaced by e .

In the mass eigenstate basis \tilde{l}_i the corresponding contribution to the branching fraction is given by:

$$\begin{aligned}
 \text{Br} \left(\tilde{l}_a \rightarrow \tilde{l}_b \gamma \right)_{\text{scalar}}^{\text{1-loop}} &\simeq \kappa \sum_{j=1}^3 \sum_{k=1}^3 \left(V_{jL}^\dagger \right)_{aj} \left[\sum_{s=1}^2 y_{js}^{(l)} x_{sk}^{(l)} (\delta_{k2} + \delta_{k3}) \right] (V_{lR})_{kb} (1 - \delta_{ab}) F_{1loop} \\
 &= \frac{\kappa}{G_{1loop} \frac{v}{\sqrt{2}}} \sum_{j=1}^3 \sum_{k=1}^3 \left(V_{jL}^\dagger \right)_{aj} M_{jk}^{(l)} (V_{lR})_{kb} (1 - \delta_{ab}) F_{1loop} \\
 &= \frac{\kappa}{G_{1loop} \frac{v}{\sqrt{2}}} \sum_{j=1}^3 \sum_{k=1}^3 (m_\mu \delta_{a2} \delta_{b2} + m_\tau \delta_{a3} \delta_{b3}) (1 - \delta_{ab}) F_{1loop} = 0, \tag{A1}
 \end{aligned}$$

what was to be shown. Here we have taken into account that the SM charged lepton mass matrix has the form:

$$M_{jk}^{(l)} = \left[\sum_{s=1}^2 y_{js}^{(l)} x_{sk}^{(l)} (\delta_{k2} + \delta_{k3}) G_{1loop} + y_j^{(l)} x_1^{(l)} \delta_{k1} G_{2loop} \right] \frac{v}{\sqrt{2}} \simeq \sum_{s=1}^2 y_{js}^{(l)} x_{sk}^{(l)} (\delta_{k2} + \delta_{k3}) G_{1loop} \frac{v}{\sqrt{2}} \tag{A2}$$

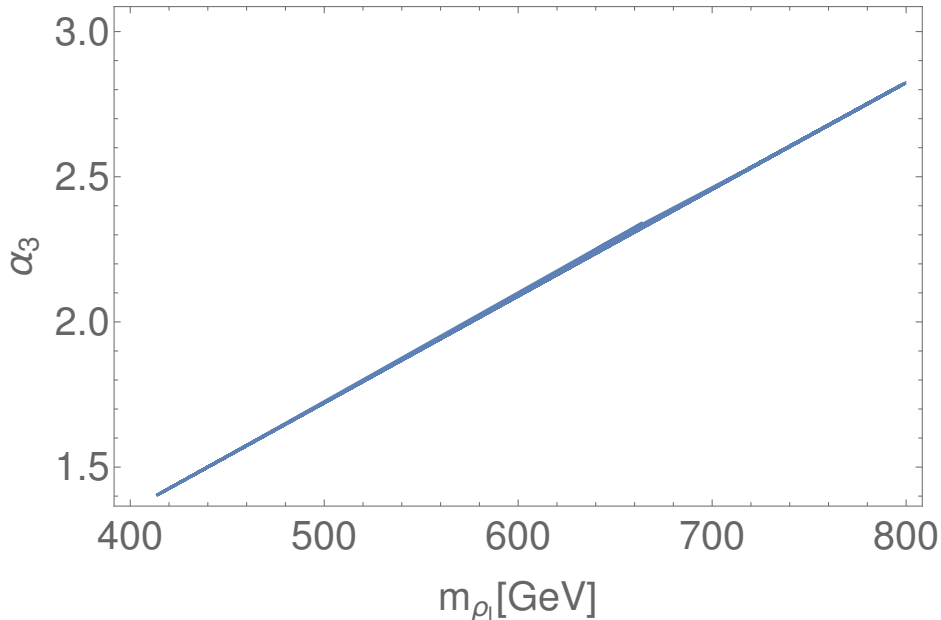


Figure 10: Correlation between the quartic scalar coupling α_3 and the mass m_{ρ_I} of the scalar Dark Matter candidate ρ_I , consistent with the experimental value $\Omega h^2 = 0.1198$ for the Relic density.

and satisfies

$$V_{jL}^\dagger M^{(l)} V_{jR} = \left(M^{(l)} \right)_{diag} \quad (\text{A3})$$

where $j, k = 1, 2, 3$, with G_{1loop} and G_{2loop} being the corresponding one and two loop functions, respectively.

The SM fermionic fields in the mass ($\tilde{f}_{(L,R)}$) and interaction ($f_{(L,R)}$) eigenstate bases are related as

$$f_{(L,R)} = V_{f(L,R)} \tilde{f}_{(L,R)}. \quad (\text{A4})$$

REFERENCES

-
- [1] B. S. Balakrishna, A. L. Kagan, and R. N. Mohapatra, “Quark Mixings and Mass Hierarchy From Radiative Corrections,” *Phys. Lett.* **B205** (1988) 345–352.
 - [2] E. Ma, “Radiative Quark and Lepton Masses Through Soft Supersymmetry Breaking,” *Phys. Rev.* **D39** (1989) 1922.
 - [3] E. Ma, D. Ng, J. T. Pantaleone, and G.-G. Wong, “One Loop Induced Fermion Masses and Exotic Interactions in a Standard Model Context,” *Phys. Rev.* **D40** (1989) 1586.
 - [4] E. Ma, “Hierarchical Radiative Quark and Lepton Mass Matrices,” *Phys. Rev. Lett.* **64** (1990) 2866–2869.
 - [5] E. Ma, “Pathways to naturally small neutrino masses,” *Phys. Rev. Lett.* **81** (1998) 1171–1174, [arXiv:hep-ph/9805219](#) [[hep-ph](#)].
 - [6] T. Kitabayashi and M. Yasue, “Radiatively induced neutrino masses and oscillations in an SU(3)(L) x U(1)(N) gauge model,” *Phys. Rev.* **D63** (2001) 095002, [arXiv:hep-ph/0010087](#) [[hep-ph](#)].
 - [7] E. Ma, “Verifiable radiative seesaw mechanism of neutrino mass and dark matter,” *Phys. Rev.* **D73** (2006) 077301, [arXiv:hep-ph/0601225](#) [[hep-ph](#)].
 - [8] P. V. Dong, D. T. Huong, T. T. Huong, and H. N. Long, “Fermion masses in the economical 3-3-1 model,” *Phys. Rev.* **D74** (2006) 053003, [arXiv:hep-ph/0607291](#) [[hep-ph](#)].

- [9] D. Chang and H. N. Long, “Interesting radiative patterns of neutrino mass in an $SU(3)(C) \times SU(3)(L) \times U(1)(X)$ model with right-handed neutrinos,” *Phys. Rev.* **D73** (2006) 053006, [arXiv:hep-ph/0603098 \[hep-ph\]](#).
- [10] P.-H. Gu and U. Sarkar, “Radiative Neutrino Mass, Dark Matter and Leptogenesis,” *Phys. Rev.* **D77** (2008) 105031, [arXiv:0712.2933 \[hep-ph\]](#).
- [11] E. Ma and D. Suematsu, “Fermion Triplet Dark Matter and Radiative Neutrino Mass,” *Mod. Phys. Lett.* **A24** (2009) 583–589, [arXiv:0809.0942 \[hep-ph\]](#).
- [12] D. Aristizabal Sierra, J. Kubo, D. Restrepo, D. Suematsu, and O. Zapata, “Radiative seesaw: Warm dark matter, collider and lepton flavour violating signals,” *Phys. Rev.* **D79** (2009) 013011, [arXiv:0808.3340 \[hep-ph\]](#).
- [13] E. Nardi, D. Restrepo, and M. Velasquez, “Neutrino Masses in $SU(5) \times U(1)_F$ with Adjoint Flavons,” *Eur. Phys. J.* **C72** (2012) 1941, [arXiv:1108.0722 \[hep-ph\]](#).
- [14] D. T. Huang, L. T. Hue, M. C. Rodriguez, and H. N. Long, “Supersymmetric reduced minimal 3-3-1 model,” *Nucl. Phys.* **B870** (2013) 293–322, [arXiv:1210.6776 \[hep-ph\]](#).
- [15] D. Restrepo, O. Zapata, and C. E. Yaguna, “Models with radiative neutrino masses and viable dark matter candidates,” *JHEP* **11** (2013) 011, [arXiv:1308.3655 \[hep-ph\]](#).
- [16] E. Ma, I. Picek, and B. Radović, “New Scotogenic Model of Neutrino Mass with $U(1)_D$ Gauge Interaction,” *Phys. Lett.* **B726** (2013) 744–746, [arXiv:1308.5313 \[hep-ph\]](#).
- [17] E. Ma, “Radiative Origin of All Quark and Lepton Masses through Dark Matter with Flavor Symmetry,” *Phys. Rev. Lett.* **112** (2014) 091801, [arXiv:1311.3213 \[hep-ph\]](#).
- [18] A. E. Carcamo Hernandez, R. Martinez, and F. Ochoa, “Radiative seesaw-type mechanism of quark masses in $SU(3)_C \otimes SU(3)_L \otimes U(1)_X$,” *Phys. Rev.* **D87** no. 7, (2013) 075009, [arXiv:1302.1757 \[hep-ph\]](#).
- [19] A. E. Carcamo Hernandez, I. de Medeiros Varzielas, S. G. Kovalenko, H. Päs, and I. Schmidt, “Lepton masses and mixings in an A_4 multi-Higgs model with a radiative seesaw mechanism,” *Phys. Rev.* **D88** no. 7, (2013) 076014, [arXiv:1307.6499 \[hep-ph\]](#).
- [20] H. Okada and K. Yagyu, “Radiative generation of lepton masses,” *Phys. Rev.* **D89** no. 5, (2014) 053008, [arXiv:1311.4360 \[hep-ph\]](#).
- [21] D. Aristizabal Sierra, A. Degee, L. Dorame, and M. Hirsch, “Systematic classification of two-loop realizations of the Weinberg operator,” *JHEP* **03** (2015) 040, [arXiv:1411.7038 \[hep-ph\]](#).
- [22] M. D. Campos, A. E. Cárcamo Hernández, S. Kovalenko, I. Schmidt, and E. Schumacher, “Fermion masses and mixings in an $SU(5)$ grand unified model with an extra flavor symmetry,” *Phys. Rev.* **D90** no. 1, (2014) 016006, [arXiv:1403.2525 \[hep-ph\]](#).
- [23] S. M. Boucenna, S. Morisi, and J. W. F. Valle, “Radiative neutrino mass in 3-3-1 scheme,” *Phys. Rev.* **D90** no. 1, (2014) 013005, [arXiv:1405.2332 \[hep-ph\]](#).
- [24] A. E. Cárcamo Hernández, “A novel and economical explanation for SM fermion masses and mixings,” *Eur. Phys. J.* **C76** no. 9, (2016) 503, [arXiv:1512.09092 \[hep-ph\]](#).
- [25] A. Aranda and E. Peinado, “A new radiative neutrino mass generation mechanism with higher dimensional scalar representations and custodial symmetry,” *Phys. Lett.* **B754** (2016) 11–13, [arXiv:1508.01200 \[hep-ph\]](#).
- [26] D. Restrepo, A. Rivera, M. Sánchez-Peláez, O. Zapata, and W. Tangarife, “Radiative Neutrino Masses in the Singlet-Doublet Fermion Dark Matter Model with Scalar Singlets,” *Phys. Rev.* **D92** no. 1, (2015) 013005, [arXiv:1504.07892 \[hep-ph\]](#).
- [27] R. Longas, D. Portillo, D. Restrepo, and O. Zapata, “The Inert Zee Model,” *JHEP* **03** (2016) 162, [arXiv:1511.01873 \[hep-ph\]](#).
- [28] S. Fraser, E. Ma, and M. Zakeri, “Verifiable Associated Processes from Radiative Lepton Masses with Dark Matter,” *Phys. Rev.* **D93** no. 11, (2016) 115019, [arXiv:1511.07458 \[hep-ph\]](#).
- [29] S. Fraser, C. Kownacki, E. Ma, and O. Popov, “Type II Radiative Seesaw Model of Neutrino Mass with Dark Matter,” *Phys. Rev.* **D93** no. 1, (2016) 013021, [arXiv:1511.06375 \[hep-ph\]](#).
- [30] H. Okada, N. Okada, and Y. Orikasa, “Radiative seesaw mechanism in a minimal 3-3-1 model,” *Phys. Rev.* **D93** no. 7, (2016) 073006, [arXiv:1504.01204 \[hep-ph\]](#).
- [31] W. Wang and Z.-L. Han, “Radiative linear seesaw model, dark matter, and $U(1)_{B-L}$,” *Phys. Rev.* **D92** (2015) 095001, [arXiv:1508.00706 \[hep-ph\]](#).
- [32] D. Aristizabal Sierra, C. Simoes, and D. Wegman, “Closing in on minimal dark matter and radiative neutrino masses,” *JHEP* **06** (2016) 108, [arXiv:1603.04723 \[hep-ph\]](#).
- [33] C. Arbeláez, A. E. Cárcamo Hernández, S. Kovalenko, and I. Schmidt, “Radiative Seesaw-type Mechanism of Fermion Masses and Non-trivial Quark Mixing,” *Eur. Phys. J.* **C77** no. 6, (2017) 422, [arXiv:1602.03607 \[hep-ph\]](#).
- [34] T. Nomura and H. Okada, “Radiatively induced Quark and Lepton Mass Model,” *Phys. Lett.* **B761** (2016) 190–196, [arXiv:1606.09055 \[hep-ph\]](#).
- [35] T. Nomura and H. Okada, “Four-loop Neutrino Model Inspired by Diphoton Excess at 750 GeV,” *Phys. Lett.* **B755** (2016) 306–311, [arXiv:1601.00386 \[hep-ph\]](#).
- [36] C. Kownacki and E. Ma, “Gauge $U(1)$ dark symmetry and radiative light fermion masses,” *Phys. Lett.* **B760** (2016) 59–62, [arXiv:1604.01148 \[hep-ph\]](#).
- [37] C. Kownacki, E. Ma, N. Pollard, and M. Zakeri, “Generalized Gauge $U(1)$ Family Symmetry for Quarks and Leptons,” *Phys. Lett.* **B766** (2017) 149–152, [arXiv:1611.05017 \[hep-ph\]](#).
- [38] T. Nomura, H. Okada, and N. Okada, “A Colored KNT Neutrino Model,” *Phys. Lett.* **B762** (2016) 409–414, [arXiv:1608.02694 \[hep-ph\]](#).
- [39] J. E. Camargo-Molina, A. P. Morais, A. Ordell, R. Pasechnik, M. O. P. Sampaio, and J. Wessén, “Reviving trinification

- models through an E6 -extended supersymmetric GUT,” *Phys. Rev.* **D95** no. 7, (2017) 075031, [arXiv:1610.03642 \[hep-ph\]](#).
- [40] J. E. Camargo-Molina, A. P. Morais, R. Pasechnik, and J. Wessén, “On a radiative origin of the Standard Model from Trification,” *JHEP* **09** (2016) 129, [arXiv:1606.03492 \[hep-ph\]](#).
- [41] F. von der Pahlen, G. Palacio, D. Restrepo, and O. Zapata, “Radiative Type III Seesaw Model and its collider phenomenology,” *Phys. Rev.* **D94** no. 3, (2016) 033005, [arXiv:1605.01129 \[hep-ph\]](#).
- [42] C. Bonilla, E. Ma, E. Peinado, and J. W. F. Valle, “Two-loop Dirac neutrino mass and WIMP dark matter,” *Phys. Lett.* **B762** (2016) 214–218, [arXiv:1607.03931 \[hep-ph\]](#).
- [43] P.-H. Gu, “High-scale leptogenesis with three-loop neutrino mass generation and dark matter,” *JHEP* **04** (2017) 159, [arXiv:1611.03256 \[hep-ph\]](#).
- [44] T. Nomura and H. Okada, “Loop induced type-II seesaw model and GeV dark matter with $U(1)_{B-L}$ gauge symmetry,” *Phys. Lett.* **B774** (2017) 575–581, [arXiv:1704.08581 \[hep-ph\]](#).
- [45] T. Nomura and H. Okada, “Radiative neutrino mass in an alternative $U(1)_{B-L}$ gauge symmetry,” *Nucl. Phys.* **B941** (2019) 586–599, [arXiv:1705.08309 \[hep-ph\]](#).
- [46] T. Nomura and H. Okada, “A model with isospin doublet $U(1)_D$ gauge symmetry,” *Int. J. Mod. Phys.* **A33** no. 14n15, (2018) 1850089, [arXiv:1706.05268 \[hep-ph\]](#).
- [47] W. Wang, R. Wang, Z.-L. Han, and J.-Z. Han, “The $B - L$ Scotogenic Models for Dirac Neutrino Masses,” *Eur. Phys. J.* **C77** no. 12, (2017) 889, [arXiv:1705.00414 \[hep-ph\]](#).
- [48] N. Bernal, A. E. Cárcamo Hernández, I. de Medeiros Varzielas, and S. Kovalenko, “Fermion masses and mixings and dark matter constraints in a model with radiative seesaw mechanism,” *JHEP* **05** (2018) 053, [arXiv:1712.02792 \[hep-ph\]](#).
- [49] A. E. Cárcamo Hernández and H. N. Long, “A highly predictive A_4 flavour 3-3-1 model with radiative inverse seesaw mechanism,” *J. Phys.* **G45** no. 4, (2018) 045001, [arXiv:1705.05246 \[hep-ph\]](#).
- [50] A. E. Cárcamo Hernández, S. Kovalenko, H. N. Long, and I. Schmidt, “A variant of 3-3-1 model for the generation of the SM fermion mass and mixing pattern,” *JHEP* **07** (2018) 144, [arXiv:1705.09169 \[hep-ph\]](#).
- [51] E. Ma and U. Sarkar, “Radiative Left-Right Dirac Neutrino Mass,” *Phys. Lett.* **B776** (2018) 54–57, [arXiv:1707.07698 \[hep-ph\]](#).
- [52] R. Cepedello, M. Hirsch, and J. C. Helo, “Loop neutrino masses from $d = 7$ operator,” *JHEP* **07** (2017) 079, [arXiv:1705.01489 \[hep-ph\]](#).
- [53] A. Dev and R. N. Mohapatra, “Natural Alignment of Quark Flavors and Radiatively Induced Quark Mixings,” *Phys. Rev.* **D98** no. 7, (2018) 073002, [arXiv:1804.01598 \[hep-ph\]](#).
- [54] A. E. Cárcamo Hernández, S. Kovalenko, J. W. F. Valle, and C. A. Vaquera-Araujo, “Neutrino predictions from a left-right symmetric flavored extension of the standard model,” *JHEP* **02** (2019) 065, [arXiv:1811.03018 \[hep-ph\]](#).
- [55] N. Rojas, R. Srivastava, and J. W. F. Valle, “Simplest Scoto-Seesaw Mechanism,” *Phys. Lett.* **B789** (2019) 132–136, [arXiv:1807.11447 \[hep-ph\]](#).
- [56] T. Nomura and H. Okada, “Zee-Babu type model with $U(1)_{L_\mu-L_\tau}$ gauge symmetry,” *Phys. Rev.* **D97** no. 9, (2018) 095023, [arXiv:1803.04795 \[hep-ph\]](#).
- [57] M. Reig, D. Restrepo, J. W. F. Valle, and O. Zapata, “Bound-state dark matter and Dirac neutrino masses,” *Phys. Rev.* **D97** no. 11, (2018) 115032, [arXiv:1803.08528 \[hep-ph\]](#).
- [58] N. Bernal, D. Restrepo, C. Yaguna, and O. Zapata, “Two-component dark matter and a massless neutrino in a new $B - L$ model,” *Phys. Rev.* **D99** no. 1, (2019) 015038, [arXiv:1808.03352 \[hep-ph\]](#).
- [59] J. Calle, D. Restrepo, C. E. Yaguna, and O. Zapata, “Minimal radiative Dirac neutrino mass models,” *Phys. Rev.* **D99** no. 7, (2019) 075008, [arXiv:1812.05523 \[hep-ph\]](#).
- [60] A. Aranda, C. Bonilla, and E. Peinado, “Dynamical generation of neutrino mass scales,” *Phys. Lett.* **B792** (2019) 40–42, [arXiv:1808.07727 \[hep-ph\]](#).
- [61] R. Cepedello, R. M. Fonseca, and M. Hirsch, “Systematic classification of three-loop realizations of the Weinberg operator,” *JHEP* **10** (2018) 197, [arXiv:1807.00629 \[hep-ph\]](#). [erratum: JHEP06,034(2019)].
- [62] A. E. Cárcamo Hernández, J. Vignatti, and A. Zerwekh, “Generating lepton masses and mixings with a heavy vector doublet,” *J. Phys.* **G46** no. 11, (2019) 115007, [arXiv:1807.05321 \[hep-ph\]](#).
- [63] E. Ma, “ $U(1)_\chi$, Seesaw Dark Matter, and Higgs Decay,” [arXiv:1810.06506 \[hep-ph\]](#).
- [64] E. Ma, “ $U(1)_\chi$ and Seesaw Dirac Neutrinos,” [arXiv:1811.09645 \[hep-ph\]](#).
- [65] S.-P. Li, X.-Q. Li, and Y.-D. Yang, “Muon $g - 2$ in a $U(1)$ -symmetric Two-Higgs-Doublet Model,” *Phys. Rev.* **D 99** no. 3, (2019) 035010, [arXiv:1808.02424 \[hep-ph\]](#).
- [66] P. Anan, A. Crivellin, M. Fedele, and F. Mescia, “Generic Loop Effects of New Scalars and Fermions in $b \rightarrow s\ell^+\ell^-$, $(g - 2)_\mu$ and a Vector-like 4th Generation,” *JHEP* **06** (2019) 118, [arXiv:1904.05890 \[hep-ph\]](#).
- [67] E. Ma, “Two-loop Z_4 Dirac neutrino masses and mixing, with self-interacting dark matter,” *Nucl. Phys.* **B946** (2019) 114725, [arXiv:1907.04665 \[hep-ph\]](#).
- [68] E. Ma, “Scotogenic cobimaximal Dirac neutrino mixing from $\Delta(27)$ and $U(1)_\chi$,” *Eur. Phys. J.* **C79** no. 11, (2019) 903, [arXiv:1905.01535 \[hep-ph\]](#).
- [69] A. E. Cárcamo Hernández, S. Kovalenko, R. Pasechnik, and I. Schmidt, “Phenomenology of an extended IDM with loop-generated fermion mass hierarchies,” *Eur. Phys. J.* **C79** no. 7, (2019) 610, [arXiv:1901.09552 \[hep-ph\]](#).
- [70] E. Ma, “Scotogenic $U(1)_\chi$ Dirac neutrinos,” *Phys. Lett.* **B793** (2019) 411–414, [arXiv:1901.09091 \[hep-ph\]](#).
- [71] T. Nomura and H. Okada, “A two loop induced neutrino mass model with modular A_4 symmetry,” *Nucl. Phys.* **B966** (2021) 115372, [arXiv:1906.03927 \[hep-ph\]](#).

- [72] T. Nomura and H. Okada, “A radiative neutrino mass model with hidden gauge symmetry inducing semi-annihilating dark matter,” [arXiv:1904.13066 \[hep-ph\]](#).
- [73] T. Nomura and H. Okada, “A modular A_4 symmetric model of dark matter and neutrino,” *Phys. Lett.* **B797** (2019) 134799, [arXiv:1904.03937 \[hep-ph\]](#).
- [74] S. Centelles Chuliá, R. Cepedello, E. Peinado, and R. Srivastava, “Scotogenic dark symmetry as a residual subgroup of Standard Model symmetries,” *Chin. Phys.* **C44** no. 8, (2020) 083110, [arXiv:1901.06402 \[hep-ph\]](#).
- [75] C. Bonilla, S. Centelles-Chuliá, R. Cepedello, E. Peinado, and R. Srivastava, “Dark matter stability and Dirac neutrinos using only Standard Model symmetries,” *Phys. Rev.* **D101** no. 3, (2020) 033011, [arXiv:1812.01599 \[hep-ph\]](#).
- [76] S. Pramanick, “Scotogenic S3 symmetric generation of realistic neutrino mixing,” *Phys. Rev.* **D100** no. 3, (2019) 035009, [arXiv:1904.07558 \[hep-ph\]](#).
- [77] C. Arbeláez, A. E. Cárcamo Hernández, R. Cepedello, M. Hirsch, and S. Kovalenko, “Radiative type-I seesaw neutrino masses,” *Phys. Rev.* **D100** no. 11, (2019) 115021, [arXiv:1910.04178 \[hep-ph\]](#).
- [78] I. M. Ávila, V. De Romeri, L. Duarte, and J. W. F. Valle, “Phenomenology of scotogenic scalar dark matter,” *Eur. Phys. J.* **C80** no. 10, (2020) 908, [arXiv:1910.08422 \[hep-ph\]](#).
- [79] A. E. Cárcamo Hernández, S. Kovalenko, R. Pasechnik, and I. Schmidt, “Sequentially loop-generated quark and lepton mass hierarchies in an extended Inert Higgs Doublet model,” *JHEP* **06** (2019) 056, [arXiv:1901.02764 \[hep-ph\]](#).
- [80] A. E. Cárcamo Hernández, D. T. Huong, and H. N. Long, “Minimal model for the fermion flavor structure, mass hierarchy, dark matter, leptogenesis, and the electron and muon anomalous magnetic moments,” *Phys. Rev.* **D102** no. 5, (2020) 055002, [arXiv:1910.12877 \[hep-ph\]](#).
- [81] C. Arbeláez, A. E. Cárcamo Hernández, R. Cepedello, S. Kovalenko, and I. Schmidt, “Sequentially loop suppressed fermion masses from a single discrete symmetry,” *JHEP* **06** (2020) 043, [arXiv:1911.02033 \[hep-ph\]](#).
- [82] A. E. Cárcamo Hernández, L. T. Hue, S. Kovalenko, and H. N. Long, “An extended 3-3-1 model with two scalar triplets and linear seesaw mechanism,” [arXiv:2001.01748 \[hep-ph\]](#).
- [83] A. E. Cárcamo Hernández, C. O. Dib, and U. J. Saldaña-Salazar, “When $\tan\beta$ meets all the mixing angles,” *Phys. Lett.* **B809** (2020) 135750, [arXiv:2001.07140 \[hep-ph\]](#).
- [84] A. E. Cárcamo Hernández, Y. Hidalgo Velásquez, S. Kovalenko, H. N. Long, N. A. Pérez-Julve, and V. V. Vien, “Fermion spectrum and $g - 2$ anomalies in a low scale 3-3-1 model,” *Eur. Phys. J.* **C81** no. 2, (2021) 191, [arXiv:2002.07347 \[hep-ph\]](#).
- [85] A. E. Cárcamo Hernández, D. T. Huong, S. Kovalenko, A. P. Morais, R. Pasechnik, and I. Schmidt, “How low-scale trification sheds light in the flavor hierarchies, neutrino puzzle, dark matter, and leptogenesis,” *Phys. Rev.* **D102** no. 9, (2020) 095003, [arXiv:2004.11450 \[hep-ph\]](#).
- [86] A. E. Cárcamo Hernández, J. W. F. Valle, and C. A. Vaquera-Araujo, “Simple theory for scotogenic dark matter with residual matter-parity,” *Phys. Lett.* **B809** (2020) 135757, [arXiv:2006.06009 \[hep-ph\]](#).
- [87] A. E. C. Hernández and I. Schmidt, “A renormalizable left-right symmetric model with low scale seesaw mechanisms,” [arXiv:2101.02718 \[hep-ph\]](#).
- [88] A. E. Cárcamo Hernández, C. Espinoza, J. Carlos Gómez-Izquierdo, and M. Mondragón, “Fermion masses and mixings, dark matter, leptogenesis and $g - 2$ muon anomaly in an extended 2HDM with inverse seesaw,” [arXiv:2104.02730 \[hep-ph\]](#).
- [89] E. Kiritsis and P. Anastopoulos, “The Anomalous magnetic moment of the muon in the D-brane realization of the standard model,” *JHEP* **05** (2002) 054, [arXiv:hep-ph/0201295](#).
- [90] T. Appelquist, M. Piai, and R. Shrock, “Lepton dipole moments in extended technicolor models,” *Phys. Lett.* **B593** (2004) 175–180, [arXiv:hep-ph/0401114 \[hep-ph\]](#).
- [91] G. F. Giudice, P. Paradisi, and M. Passera, “Testing new physics with the electron $g-2$,” *JHEP* **11** (2012) 113, [arXiv:1208.6583 \[hep-ph\]](#).
- [92] Y. Omura, E. Senaha, and K. Tobe, “Lepton-flavor-violating Higgs decay $h \rightarrow \mu\tau$ and muon anomalous magnetic moment in a general two Higgs doublet model,” *JHEP* **05** (2015) 028, [arXiv:1502.07824 \[hep-ph\]](#).
- [93] A. Falkowski, S. F. King, E. Perdomo, and M. Pierre, “Flavourful Z' portal for vector-like neutrino Dark Matter and $R_{K^{(*)}}$,” *JHEP* **08** (2018) 061, [arXiv:1803.04430 \[hep-ph\]](#).
- [94] A. Crivellin, M. Hoferichter, and P. Schmidt-Wellenburg, “Combined explanations of $(g - 2)_{\mu,e}$ and implications for a large muon EDM,” *Phys. Rev.* **D98** no. 11, (2018) 113002, [arXiv:1807.11484 \[hep-ph\]](#).
- [95] B. Allanach, F. S. Queiroz, A. Strumia, and S. Sun, “ Z' models for the LHCb and $g - 2$ muon anomalies,” *Phys. Rev.* **D93** no. 5, (2016) 055045, [arXiv:1511.07447 \[hep-ph\]](#). [Erratum: *Phys. Rev.* **D95**, no. 11, 119902 (2017)].
- [96] B. P. Padley, K. Sinha, and K. Wang, “Natural Supersymmetry, Muon $g - 2$, and the Last Crevices for the Top Squark,” *Phys. Rev.* **D92** no. 5, (2015) 055025, [arXiv:1505.05877 \[hep-ph\]](#).
- [97] C.-H. Chen, T. Nomura, and H. Okada, “Explanation of $B \rightarrow K^{(*)} \ell^+ \ell^-$ and muon $g - 2$, and implications at the LHC,” *Phys. Rev.* **D94** no. 11, (2016) 115005, [arXiv:1607.04857 \[hep-ph\]](#).
- [98] S. Raby and A. Trautner, “Vectorlike chiral fourth family to explain muon anomalies,” *Phys. Rev.* **D97** no. 9, (2018) 095006, [arXiv:1712.09360 \[hep-ph\]](#).
- [99] C.-W. Chiang, H. Okada, and E. Senaha, “Dark matter, muon $g - 2$, electric dipole moments, and $Z \rightarrow \ell_i^+ \ell_j^-$ in a one-loop induced neutrino model,” *Phys. Rev.* **D96** no. 1, (2017) 015002, [arXiv:1703.09153 \[hep-ph\]](#).
- [100] C.-H. Chen, T. Nomura, and H. Okada, “Excesses of muon $g - 2$, $R_{D^{(*)}}$, and R_K in a leptoquark model,” *Phys. Lett.* **B774** (2017) 456–464, [arXiv:1703.03251 \[hep-ph\]](#).
- [101] E. Megias, M. Quiros, and L. Salas, “ $g_\mu - 2$ from Vector-Like Leptons in Warped Space,” *JHEP* **05** (2017) 016,

- arXiv:1701.05072 [hep-ph].
- [102] H. Davoudiasl and W. J. Marciano, “Tale of two anomalies,” *Phys. Rev.* **D98** no. 7, (2018) 075011, arXiv:1806.10252 [hep-ph].
- [103] J. Liu, C. E. M. Wagner, and X.-P. Wang, “A light complex scalar for the electron and muon anomalous magnetic moments,” *JHEP* **03** (2019) 008, arXiv:1810.11028 [hep-ph].
- [104] T. Nomura and H. Okada, “Muon anomalous magnetic moment, Z boson decays, and collider physics in multicharged particles,” *Phys. Rev.* **D101** no. 1, (2020) 015021, arXiv:1903.05958 [hep-ph].
- [105] J. Kawamura, S. Raby, and A. Trautner, “Complete vectorlike fourth family and new $U(1)'$ for muon anomalies,” *Phys. Rev.* **D100** no. 5, (2019) 055030, arXiv:1906.11297 [hep-ph].
- [106] M. Bauer, M. Neubert, S. Renner, M. Schnubel, and A. Thamm, “Axionlike Particles, Lepton-Flavor Violation, and a New Explanation of a_μ and a_e ,” *Phys. Rev. Lett.* **124** no. 21, (2020) 211803, arXiv:1908.00008 [hep-ph].
- [107] F. J. Botella, F. Cornet-Gomez, and M. Nebot, “Flavor conservation in two-Higgs-doublet models,” *Phys. Rev.* **D98** no. 3, (2018) 035046, arXiv:1803.08521 [hep-ph].
- [108] X.-F. Han, T. Li, L. Wang, and Y. Zhang, “Simple interpretations of lepton anomalies in the lepton-specific inert two-Higgs-doublet model,” *Phys. Rev.* **D99** no. 9, (2019) 095034, arXiv:1812.02449 [hep-ph].
- [109] L. Wang, J. M. Yang, M. Zhang, and Y. Zhang, “Revisiting lepton-specific 2HDM in light of muon $g - 2$ anomaly,” *Phys. Lett.* **B788** (2019) 519–529, arXiv:1809.05857 [hep-ph].
- [110] B. Dutta and Y. Mimura, “Electron $g - 2$ with flavor violation in MSSM,” *Phys. Lett.* **B790** (2019) 563–567, arXiv:1811.10209 [hep-ph].
- [111] M. Badziak and K. Sakurai, “Explanation of electron and muon $g - 2$ anomalies in the MSSM,” *JHEP* **10** (2019) 024, arXiv:1908.03607 [hep-ph].
- [112] M. Endo and W. Yin, “Explaining electron and muon $g - 2$ anomaly in SUSY without lepton-flavor mixings,” *JHEP* **08** (2019) 122, arXiv:1906.08768 [hep-ph].
- [113] G. Hiller, C. Hormigos-Feliu, D. F. Litim, and T. Steudtner, “Anomalous magnetic moments from asymptotic safety,” *Phys. Rev.* **D102** no. 7, (2020) 071901, arXiv:1910.14062 [hep-ph].
- [114] A. E. Cárcamo Hernández, S. F. King, H. Lee, and S. J. Rowley, “Is it possible to explain the muon and electron $g - 2$ in a Z' model?,” *Phys. Rev.* **D101** no. 11, (2020) 115016, arXiv:1910.10734 [hep-ph].
- [115] J. Kawamura, S. Raby, and A. Trautner, “Complete vectorlike fourth family with $U(1)'$: A global analysis,” *Phys. Rev.* **D101** no. 3, (2020) 035026, arXiv:1911.11075 [hep-ph].
- [116] D. Sabatta, A. S. Cornell, A. Goyal, M. Kumar, B. Mellado, and X. Ruan, “Connecting muon anomalous magnetic moment and multi-lepton anomalies at LHC,” *Chin. Phys.* **C44** no. 6, (2020) 063103, arXiv:1909.03969 [hep-ph].
- [117] K.-F. Chen, C.-W. Chiang, and K. Yagyu, “An explanation for the muon and electron $g - 2$ anomalies and dark matter,” *JHEP* **09** (2020) 119, arXiv:2006.07929 [hep-ph].
- [118] S. Iguro, Y. Omura, and M. Takeuchi, “Testing the 2HDM explanation of the muon $g - 2$ anomaly at the LHC,” *JHEP* **11** (2019) 130, arXiv:1907.09845 [hep-ph].
- [119] S.-P. Li, X.-Q. Li, Y.-Y. Li, Y.-D. Yang, and X. Zhang, “Power-aligned 2HDM: a correlative perspective on $(g - 2)_{e,\mu}$,” *JHEP* **01** (2021) 034, arXiv:2010.02799 [hep-ph].
- [120] C. Arbeláez, R. Cepedello, R. M. Fonseca, and M. Hirsch, “ $(g - 2)$ anomalies and neutrino mass,” *Phys. Rev.* **D102** no. 7, (2020) 075005, arXiv:2007.11007 [hep-ph].
- [121] G. Hiller, C. Hormigos-Feliu, D. F. Litim, and T. Steudtner, “Model Building from Asymptotic Safety with Higgs and Flavor Portals,” *Phys. Rev.* **D102** no. 9, (2020) 095023, arXiv:2008.08606 [hep-ph].
- [122] S. Jana, V. P. K., and S. Saad, “Resolving electron and muon $g - 2$ within the 2HDM,” *Phys. Rev.* **D101** no. 11, (2020) 115037, arXiv:2003.03386 [hep-ph].
- [123] A. S. de Jesus, S. Kovalenko, C. A. de S. Pires, F. S. Queiroz, and Y. S. Villamizar, “Dead or alive? Implications of the muon anomalous magnetic moment for 3-3-1 models,” *Phys. Lett.* **B809** (2020) 135689, arXiv:2003.06440 [hep-ph].
- [124] A. S. De Jesus, S. Kovalenko, F. S. Queiroz, C. Siqueira, and K. Sinha, “Vectorlike leptons and inert scalar triplet: Lepton flavor violation, $g - 2$, and collider searches,” *Phys. Rev.* **D102** no. 3, (2020) 035004, arXiv:2004.01200 [hep-ph].
- [125] C. Hati, J. Kriewald, J. Orloff, and A. M. Teixeira, “Anomalies in ^8Be nuclear transitions and $(g - 2)_{e,\mu}$: towards a minimal combined explanation,” *JHEP* **07** (2020) 235, arXiv:2005.00028 [hep-ph].
- [126] F. J. Botella, F. Cornet-Gomez, and M. Nebot, “Electron and muon $g - 2$ anomalies in general flavour conserving two Higgs doublets models,” *Phys. Rev.* **D102** no. 3, (2020) 035023, arXiv:2006.01934 [hep-ph].
- [127] I. Doršner, S. Fajfer, and S. Saad, “ $\mu \rightarrow e\gamma$ selecting scalar leptoquark solutions for the $(g - 2)_{e,\mu}$ puzzles,” *Phys. Rev.* **D102** no. 7, (2020) 075007, arXiv:2006.11624 [hep-ph].
- [128] L. Calibbi, M. L. López-Ibáñez, A. Melis, and O. Vives, “Muon and electron $g - 2$ and lepton masses in flavor models,” *JHEP* **06** (2020) 087, arXiv:2003.06633 [hep-ph].
- [129] L. T. Hue, P. N. Thanh, and T. D. Tham, “Anomalous Magnetic Dipole Moment $(g - 2)_\mu$ in 3-3-1 Model with Inverse Seesaw Neutrinos,” *Commun.in Phys.* **30** no. 3, (2020) 221–230.
- [130] S. Jana, P. K. Vishnu, W. Rodejohann, and S. Saad, “Dark matter assisted lepton anomalous magnetic moments and neutrino masses,” *Phys. Rev.* **D102** no. 7, (2020) 075003, arXiv:2008.02377 [hep-ph].
- [131] E. J. Chun and T. Mondal, “Explaining $g - 2$ anomalies in two Higgs doublet model with vector-like leptons,” *JHEP* **11** (2020) 077, arXiv:2009.08314 [hep-ph].
- [132] C.-K. Chua, “Data-driven study of the implications of anomalous magnetic moments and lepton flavor violating processes of e , μ and τ ,” *Phys. Rev.* **D102** no. 5, (2020) 055022, arXiv:2004.11031 [hep-ph].

- [133] Y. Daikoku and H. Okada, “Lepton Anomalous Magnetic Moments in an S_4 Flavor-Symmetric Extra $U(1)$ Model,” [arXiv:2011.10374 \[hep-ph\]](#).
- [134] H. Banerjee, B. Dutta, and S. Roy, “Supersymmetric gauged $U(1)_{L_\mu-L_\tau}$ model for electron and muon ($g-2$) anomaly,” *JHEP* **03** (2021) 211, [arXiv:2011.05083 \[hep-ph\]](#).
- [135] C.-H. Chen and T. Nomura, “Electron and muon $g-2$, radiative neutrino mass, and $\ell' \rightarrow \ell\gamma$ in a $U(1)_{e-\mu}$ model,” *Nucl. Phys.* **B964** (2021) 115314, [arXiv:2003.07638 \[hep-ph\]](#).
- [136] I. Bigaran and R. R. Volkas, “Getting chirality right: Single scalar leptoquark solutions to the $(g-2)_{e,\mu}$ puzzle,” *Phys. Rev.* **D102** no. 7, (2020) 075037, [arXiv:2002.12544 \[hep-ph\]](#).
- [137] J. Kawamura, S. Okawa, and Y. Omura, “Current status and muon $g-2$ explanation of lepton portal dark matter,” *JHEP* **08** (2020) 042, [arXiv:2002.12534 \[hep-ph\]](#).
- [138] M. Endo, S. Iguro, and T. Kitahara, “Probing $e\mu$ flavor-violating ALP at Belle II,” *JHEP* **06** (2020) 040, [arXiv:2002.05948 \[hep-ph\]](#).
- [139] S. Iguro, Y. Omura, and M. Takeuchi, “Probing $\mu\tau$ flavor-violating solutions for the muon $g-2$ anomaly at Belle II,” *JHEP* **09** (2020) 144, [arXiv:2002.12728 \[hep-ph\]](#).
- [140] W. Yin and M. Yamaguchi, “Muon $g-2$ at multi-TeV muon collider,” [arXiv:2012.03928 \[hep-ph\]](#).
- [141] N. Chen, B. Wang, and C.-Y. Yao, “The collider tests of a leptophilic scalar for the anomalous magnetic moments,” [arXiv:2102.05619 \[hep-ph\]](#).
- [142] P. Athron, C. Balázs, D. H. Jacob, W. Kotlarski, D. Stöckinger, and H. Stöckinger-Kim, “New physics explanations of a_μ in light of the FNAL muon $g-2$ measurement,” [arXiv:2104.03691 \[hep-ph\]](#).
- [143] G. Arcadi, L. Calibbi, M. Fedele, and F. Mescia, “Muon $g-2$ and B -anomalies from Dark Matter,” [arXiv:2104.03228 \[hep-ph\]](#).
- [144] P. Das, M. Kumar Das, and N. Khan, “The FIMP-WIMP dark matter and Muon $g-2$ in the extended singlet scalar model,” [arXiv:2104.03271 \[hep-ph\]](#).
- [145] W. Yin and W. Yin, “Radiative lepton mass and muon $g-2$ with suppressed lepton flavor and CP violations,” [arXiv:2103.14234 \[hep-ph\]](#).
- [146] W. Yin, “Muon $g-2$ Anomaly in Anomaly Mediation,” [arXiv:2104.03259 \[hep-ph\]](#).
- [147] C.-W. Chiang and K. Yagyu, “Radiative Seesaw Mechanism for Charged Leptons,” [arXiv:2104.00890 \[hep-ph\]](#).
- [148] P. Escribano, J. Terol-Calvo, and A. Vicente, “ $(g-2)_{e,\mu}$ in an extended inverse type-III seesaw,” [arXiv:2104.03705 \[hep-ph\]](#).
- [149] H.-B. Zhang, C.-X. Liu, J.-L. Yang, and T.-F. Feng, “Muon anomalous magnetic dipole moment in the $\mu\nu$ SSM,” [arXiv:2104.03489 \[hep-ph\]](#).
- [150] J.-L. Yang, H.-B. Zhang, C.-X. Liu, X.-X. Dong, and T.-F. Feng, “Muon $(g-2)$ in the B-LSSM,” [arXiv:2104.03542 \[hep-ph\]](#).
- [151] T. Li, M. A. Schmidt, C.-Y. Yao, and M. Yuan, “Charged lepton flavor violation in light of the muon magnetic moment anomaly and colliders,” [arXiv:2104.04494 \[hep-ph\]](#).
- [152] A. E. C. Hernández, S. F. King, and H. Lee, “Fermion mass hierarchies from vector-like families with an extended 2HDM and a possible explanation for the electron and muon anomalous magnetic moments,” [arXiv:2101.05819 \[hep-ph\]](#).
- [153] A. E. C. Hernández, H. N. Long, M. L. Mora-Urrutia, N. H. Thao, and V. V. Vien, “Fermion masses and mixings and $g-2$ muon anomaly in a 3-3-1 model with D_4 family symmetry,” [arXiv:2104.04559 \[hep-ph\]](#).
- [154] Muon $g-2$ Collaboration, B. Abi *et al.*, “Measurement of the Positive Muon Anomalous Magnetic Moment to 0.46 ppm,” *Phys. Rev. Lett.* **126** no. 14, (2021) 141801, [arXiv:2104.03281 \[hep-ex\]](#).
- [155] A. E. Cárcamo Hernández, S. Kovalenko, and I. Schmidt, “Radiatively generated hierarchy of lepton and quark masses,” *JHEP* **02** (2017) 125, [arXiv:1611.09797 \[hep-ph\]](#).
- [156] A. Ibarra and A. Solaguren-Beascoa, “Radiative Generation of Quark Masses and Mixing Angles in the Two Higgs Doublet Model,” *Phys. Lett.* **B736** (2014) 16–19, [arXiv:1403.2382 \[hep-ph\]](#).
- [157] W. Altmannshofer, C. Frugiuele, and R. Harnik, “Fermion Hierarchy from Sfermion Anarchy,” *JHEP* **12** (2014) 180, [arXiv:1409.2522 \[hep-ph\]](#).
- [158] G. L. Fogli, E. Lisi, A. Marrone, and G. Scioscia, “Super-Kamiokande atmospheric neutrino data, zenith distributions, and three flavor oscillations,” *Phys. Rev.* **D59** (1999) 033001, [arXiv:hep-ph/9808205 \[hep-ph\]](#).
- [159] M. Maniatis and O. Nachtmann, “Stability and symmetry breaking in the general three-Higgs-doublet model,” *JHEP* **02** (2015) 058, [arXiv:1408.6833 \[hep-ph\]](#). [Erratum: *JHEP*10,149(2015)].
- [160] M. Maniatis, A. von Manteuffel, and O. Nachtmann, “Determining the global minimum of Higgs potentials via Groebner bases: Applied to the NMSSM,” *Eur. Phys. J.* **C49** (2007) 1067–1076, [arXiv:hep-ph/0608314 \[hep-ph\]](#).
- [161] C. C. Nishi, “CP violation conditions in N-Higgs-doublet potentials,” *Phys. Rev.* **D74** (2006) 036003, [arXiv:hep-ph/0605153 \[hep-ph\]](#). [Erratum: *Phys. Rev.*D76,119901(2007)].
- [162] M. Maniatis, A. von Manteuffel, O. Nachtmann, and F. Nagel, “Stability and symmetry breaking in the general two-Higgs-doublet model,” *Eur. Phys. J.* **C48** (2006) 805–823, [arXiv:hep-ph/0605184 \[hep-ph\]](#).
- [163] M. Maniatis and D. Mehta, “Minimizing Higgs Potentials via Numerical Polynomial Homotopy Continuation,” *Eur. Phys. J. Plus* **127** (2012) 91, [arXiv:1203.0409 \[hep-ph\]](#).
- [164] A. Leykin, J. Verschelde, and Y. Zhuang, “Parallel homotopy algorithms to solve polynomial systems,” 2006.
- [165] Z.-z. Xing, “Flavor structures of charged fermions and massive neutrinos,” *Phys. Rept.* **854** (2020) 1–147, [arXiv:1909.09610 \[hep-ph\]](#).
- [166] Particle Data Group Collaboration, M. Tanabashi *et al.*, “Review of Particle Physics,” *Phys. Rev.* **D98** no. 3, (2018)

- 030001.
- [167] E. Ma and M. Raidal, “Neutrino mass, muon anomalous magnetic moment, and lepton flavor nonconservation,” *Phys. Rev. Lett.* **87** (2001) 011802, [arXiv:hep-ph/0102255 \[hep-ph\]](#). [Erratum: *Phys. Rev. Lett.* 87,159901(2001)].
 - [168] T. Toma and A. Vicente, “Lepton Flavor Violation in the Scotogenic Model,” *JHEP* **01** (2014) 160, [arXiv:1312.2840 \[hep-ph\]](#).
 - [169] A. Vicente and C. E. Yaguna, “Probing the scotogenic model with lepton flavor violating processes,” *JHEP* **02** (2015) 144, [arXiv:1412.2545 \[hep-ph\]](#).
 - [170] M. Lindner, M. Platscher, and F. S. Queiroz, “A Call for New Physics : The Muon Anomalous Magnetic Moment and Lepton Flavor Violation,” *Phys. Rept.* **731** (2018) 1–82, [arXiv:1610.06587 \[hep-ph\]](#).
 - [171] R. H. Bernstein and P. S. Cooper, “Charged Lepton Flavor Violation: An Experimenter’s Guide,” *Phys. Rept.* **532** (2013) 27–64, [arXiv:1307.5787 \[hep-ex\]](#).
 - [172] Y. Kuno and Y. Okada, “Muon decay and physics beyond the standard model,” *Rev. Mod. Phys.* **73** (2001) 151–202, [arXiv:hep-ph/9909265 \[hep-ph\]](#).
 - [173] J. Aysto *et al.*, “Physics with low-energy muons at a neutrino factory complex,” [arXiv:hep-ph/0109217 \[hep-ph\]](#).
 - [174] K. Hagiwara, R. Liao, A. D. Martin, D. Nomura, and T. Teubner, “ $(g - 2)_\mu$ and $\alpha(M_Z^2)$ re-evaluated using new precise data,” *J. Phys.* **G38** (2011) 085003, [arXiv:1105.3149 \[hep-ph\]](#).
 - [175] M. Davier, A. Hoecker, B. Malaescu, and Z. Zhang, “Reevaluation of the hadronic vacuum polarisation contributions to the Standard Model predictions of the muon $g - 2$ and $\alpha(m_Z^2)$ using newest hadronic cross-section data,” *Eur. Phys. J.* **C77** no. 12, (2017) 827, [arXiv:1706.09436 \[hep-ph\]](#).
 - [176] T. Nomura and H. Okada, “One-loop neutrino mass model without any additional symmetries,” *Phys. Dark Univ.* **26** (2019) 100359, [arXiv:1808.05476 \[hep-ph\]](#).
 - [177] **RBC, UKQCD** Collaboration, T. Blum, P. A. Boyle, V. Gülpers, T. Izubuchi, L. Jin, C. Jung, A. Jüttner, C. Lehner, A. Portelli, and J. T. Tsang, “Calculation of the hadronic vacuum polarization contribution to the muon anomalous magnetic moment,” *Phys. Rev. Lett.* **121** no. 2, (2018) 022003, [arXiv:1801.07224 \[hep-lat\]](#).
 - [178] A. Keshavarzi, D. Nomura, and T. Teubner, “Muon $g - 2$ and $\alpha(M_Z^2)$: a new data-based analysis,” *Phys. Rev.* **D97** no. 11, (2018) 114025, [arXiv:1802.02995 \[hep-ph\]](#).
 - [179] T. Aoyama *et al.*, “The anomalous magnetic moment of the muon in the Standard Model,” *Phys. Rept.* **887** (2020) 1–166, [arXiv:2006.04822 \[hep-ph\]](#).
 - [180] R. H. Parker, C. Yu, W. Zhong, B. Estey, and H. Müller, “Measurement of the fine-structure constant as a test of the Standard Model,” *Science* **360** (2018) 191, [arXiv:1812.04130 \[physics.atom-ph\]](#).
 - [181] L. Morel, Z. Yao, P. Cladé, and S. Guellati-Khélifa, “Determination of the fine-structure constant with an accuracy of 81 parts per trillion,” *Nature* **588** no. 7836, (2020) 61–65.
 - [182] **Muon g-2** Collaboration, G. W. Bennett *et al.*, “Final Report of the Muon E821 Anomalous Magnetic Moment Measurement at BNL,” *Phys. Rev. D* **73** (2006) 072003, [arXiv:hep-ex/0602035](#).
 - [183] R. A. Diaz, R. Martinez, and J. A. Rodriguez, “Phenomenology of lepton flavor violation in 2HDM(3) from $(g-2)(\mu)$ and leptonic decays,” *Phys. Rev.* **D67** (2003) 075011, [arXiv:hep-ph/0208117 \[hep-ph\]](#).
 - [184] F. Jegerlehner and A. Nyffeler, “The Muon $g-2$,” *Phys. Rept.* **477** (2009) 1–110, [arXiv:0902.3360 \[hep-ph\]](#).
 - [185] C. Kelso, H. N. Long, R. Martinez, and F. S. Queiroz, “Connection of $g - 2_\mu$, electroweak, dark matter, and collider constraints on 331 models,” *Phys. Rev.* **D90** no. 11, (2014) 113011, [arXiv:1408.6203 \[hep-ph\]](#).
 - [186] K. Kowalska and E. M. Sessolo, “Expectations for the muon $g-2$ in simplified models with dark matter,” *JHEP* **09** (2017) 112, [arXiv:1707.00753 \[hep-ph\]](#).
 - [187] J. Edsjo and P. Gondolo, “Neutralino relic density including coannihilations,” *Phys. Rev.* **D56** (1997) 1879–1894, [arXiv:hep-ph/9704361 \[hep-ph\]](#).
 - [188] S. Bhattacharya, P. Poullose, and P. Ghosh, “Multipartite Interacting Scalar Dark Matter in the light of updated LUX data,” *JCAP* **1704** (2017) 043, [arXiv:1607.08461 \[hep-ph\]](#).
 - [189] **Planck** Collaboration, P. A. R. Ade *et al.*, “Planck 2015 results. XIII. Cosmological parameters,” *Astron. Astrophys.* **594** (2016) A13, [arXiv:1502.01589 \[astro-ph.CO\]](#).